AD-A081 944 CIVIL ENGINEERING LAB (NAVY) PORT HUENEME CA F/G 8/13
SEISMIC SOIL LIQUEFACTION STUDIES.(U)
DEC 79 J B FORREST, J M FERRITTO, G WU
UNCLASSIFIED CEL-TN-1566 NL

1 OF 1
AD
A081944

END
DATE
FILMED
4-80
DTIC

12

LEVEL II

Technical Note

CEL

TN no. N-1566

title: SEISMIC SOIL LIQUEFACTION STUDIES

author: J. B. Forrest, J. M. Ferritto, and G. Wu

date: December 1979

sponsor: Naval Facilities Engineering Command

program nos: YF53.534.091.01.402

CIVIL ENGINEERING LABORATORY
NAVAL CONSTRUCTION BATTALION CENTER
Port Hueneme, California 93043

Unclassified

SECURITY CLASSIFICATION OF THIS PAGE (When Data Entered)

REPORT DOCUMENTATION PAGE		READ INSTRUCTIONS BEFORE COMPLETING FORM
1. REPORT NUMBER TN-1566	2. GOVT ACCESSION NO. DN687101	3. ~~RECIPIENT'S CATALOG NUMBER~~ Repti
4. TITLE (and Subtitle) 6 SEISMIC SOIL LIQUEFACTION STUDIES		5. ~~TYPE OF REPORT & PERIOD COVERED~~ 9 Final Oct [redacted]78 – Oct [redacted]79 6. ~~PERFORMING ORG. REPORT NUMBER~~
7. AUTHOR(s) 10 J. B. Forrest, J. M. Ferritto [redacted] G. Wu		8. CONTRACT OR GRANT NUMBER(s) 12 38
9. PERFORMING ORGANIZATION NAME AND ADDRESS CIVIL ENGINEERING LABORATORY Naval Construction Battalion Center Port Hueneme, California 93043		10. PROGRAM ELEMENT, PROJECT, TASK AREA & WORK UNIT NUMBERS YF53.534.091.01.402
11. CONTROLLING OFFICE NAME AND ADDRESS Naval Facilities Engineering Command Alexandria, Virginia 22332		12. ~~REPORT DATE~~ 11 Dec [redacted]79 13. ~~NUMBER OF PAGES~~ 34
14. MONITORING AGENCY NAME & ADDRESS (if different from Controlling Office) 16 F53534		15. SECURITY CLASS. (of this report) Unclassified 15a. DECLASSIFICATION DOWNGRADING SCHEDULE

16. DISTRIBUTION STATEMENT (of this Report)

17 YF53534091

Approved for public release; distribution unlimited.

17. DISTRIBUTION STATEMENT (of the abstract entered in Block 20, if different from Report)

14 CEL-TN-1566 391 111

18. SUPPLEMENTARY NOTES

19. KEY WORDS (Continue on reverse side if necessary and identify by block number)

Liquefaction, earthquakes, soils, waterfront, cyclic triaxial testing, cone penetrometer, pore pressure, computer codes, soil reconnaissance, piezometers.

20. ABSTRACT (Continue on reverse side if necessary and identify by block number)

Earthquake-induced soil liquefaction is considered from the points of view of site evaluation technology, and computer-based analytical developments. In-situ expedient testing procedures are compared with the results of laboratory testing on undisturbed samples. Several types of friction cone penetrometer tests are described, and mechanical cone, electrical cone, and piezometric cone sounding data are compared. Recent developments on analytical effective stress soil models are discussed. over cont.

DD FORM 1473 1 JAN 73 EDITION OF 1 NOV 65 IS OBSOLETE

Unclassified

SECURITY CLASSIFICATION OF THIS PAGE (When Data Entered)

391111

Unclassified
SECURITY CLASSIFICATION OF THIS PAGE(When Data Entered)

20. Continued

Liquefaction behavior is separated into two categories: (1) the inherently unstable situation wherein in-situ stress exceeds residual strength, and (2) the case where accumulation of deformation reaches unacceptable levels. It is suggested that the accumulated deformations category cannot be adequately evaluated using available experimental procedures, but must depend upon effective stress soil model development.

Library Card

Civil Engineering Laboratory
SEISMIC SOIL LIQUEFACTION STUDIES (Final), by
J. B. Forrest, J. M. Ferritto, & G. Wu
TN-1566 34 pp illus December 1979 Unclassified

1. Soil liquefaction 2. Earthquakes I. YF53.534.091.01.402

Earthquake-induced soil liquefaction is considered from the points of view of site evaluation technology, and computer-based analytical developments. In-situ expedient testing procedures are compared with the results of laboratory testing on undisturbed samples. Several types of friction cone penetrometer tests are described, and mechanical cone, electrical cone, and piezometric cone sounding data are compared. Recent developments on analytical effective stress soil models are discussed.

Liquefaction behavior is separated into two categories: (1) the inherently unstable situation wherein in-situ stress exceeds residual strength, and (2) the case where accumulation of deformation reaches unacceptable levels. It is suggested that the accumulated deformations category cannot be adequately evaluated using available experimental procedures, but must depend upon effective stress soil model development.

Unclassified
SECURITY CLASSIFICATION OF THIS PAGE(When Data Entered)

CONTENTS

INTRODUCTION

This report is the second interim report outlining accomplishments on a research project aimed at reduction of the earthquake-induced liquefaction hazard at Naval Shore Facilities. The previous report (Ref 1) provided a basic background on the liquefaction problem with respect to Navy requirements and summarized the goals and directions of research to be pursued. As stated in Reference 1, this study was directed largely toward monitoring the overall field of liquefaction analysis in order that the most appropriate emerging techniques be recognized for further development or adaption to Navy purposes.

Two main aspects of liquefaction development are being considered: (1) site evaluation technology and (2) analytical techniques.

Reference 2 was prepared and distributed as part of this project to serve as an interim guide summarizing current engineering practice for assessing liquefaction potential. Major deficiencies exist in current technology, particularly in determining the occurrence of liquefaction in other than level ground (no structure) situations. Further, the procedures for estimation of structural behavior - given the occurrence of site liquefaction - are not well established. Thus, the focus of this effort is twofold: (1) to evaluate the prediction of the occurrence of liquefaction by the best field and laboratory techniques, and (2) given the occurrence of an increase in pore pressure, to evaluate its effect on the structure. To accomplish this latter goal, emphasis has been placed on developing effective stress analytical material models.

Field work has continued at the Naval Air Station (NAS) North Island, including electric friction cone probings and piezometric cone soundings; and in-house cyclic triaxial testing of North Island soils has commenced. These items are further discussed in later sections of this report.

TECHNOLOGY SUMMARY

During the past several years new terminology has developed with respect to liquefaction of soils, and this has led to the potential for misunderstanding and misinterpretation. In order to clarify this situation, the Committee on Soil Dynamics of the Geotechnical Division of the American Society of Civil Engineers has prepared a list of recommended definitions (Ref 3).

The suggested terminology applies the term "liquefaction" to the situation wherein a soil is transformed into a transient liquefied state, regardless of the initiating disturbance. The use of modifiers

such as "cyclic" liquefaction, "initial" liquefaction, etc., are discouraged. The situation of progressively increasing strain-to-stress ratios that occurs during cyclic loading is referred to as "cyclic strain softening."

A generated pore pressure increment equal to the effective confining pressure that existed prior to commencement of dynamic loading is referred to as "full or 100% pore pressure ratio" (rather than "initial liquefaction," as was used formerly).

Distinction is made between "shear strength" and "shear resistance." For example, shear strength is defined as the maximum resistance of soil to shearing stresses. "Cyclic shear resistance" is the level of cyclic stress required to produce a given strain (or liquefaction) in a specified number of load cycles.

"Limited flow strain" or "limited flow deformation" occurs following transient liquefaction, prior to recovery of resistance due to dilatency. "Unlimited flow strain" or "unlimited flow deformations" continue unabated under undrained stress and are accompanied by permanent loss of shear strength.

Traditionally, liquefaction has been defined as the situation involving unrecoverable loss of resistance to deformation caused by buildup of high pore water pressures.

According to Castro (Refs 4,5), any soil whose ultimate undrained residual strength is less than the in situ shear stresses is unstable. The undrained shear strength is assumed to be a function of only the initial soil state and independent of the way in which the failure load is applied. This means that the unlimited flow threat can be evaluated in terms of two factors: (1) the undrained residual shear strength and (2) the in situ stress state.

Thus, the major difficulty in analyzing cohesionless soils with respect to earthquake loading would appear to be in the prediction of strain accumulation; i.e., the cyclic shear resistance.

As has been noted by Finn (Ref 6), unless stress reversals occur in a cyclically loaded soil specimen, pore pressure buildup may never rise to the level of confining pressure (formerly called initial liquefaction). Nevertheless, very large accumulation of strain may occur under stress levels that are below the static shear strength.

In light of the above, experimental evaluations of the liquefaction hazard appear to fall into two areas. The first area is theoretically trivial, in that any situation wherein field stress exceeds residual undrained strength is unstable and cannot be tolerated. (This still offers problems in practice in that a valid evaluation of the residual strength and in situ shear stress may be difficult.) The second area, that of assessing strain, becomes almost intractable in that as soon as large strain accumulations commence in a laboratory specimen, the validity of the test results becomes subject to question (Refs 4,7).

The foregoing is not offered as an argument against cyclic testing of soils in the laboratory, but rather to emphasize the degree of judgment that is still necessary in geotechnical earthquake engineering. This judgment becomes even more important with regard to complex waterfront

construction. For example, it is shown (Ref 8) that earth dams, which are relatively forgiving as far as deformation is concerned, generally stand up to earthquakes quite well. Thus, only in cases of poorly constructed, saturated, cohesionless materials or under unusually severe ground motions do earth dams generally undergo major earthquake damage. However, soil retaining structures, such as are prevalent at the waterfront, have wide ranges of deformation acceptability. Some structures, such as sheet pile cells or drydock walls, may fail under relatively minor dislocations, whereas relieving platforms, tied bulkhead walls, etc., in some cases may permit relatively large deformations prior to functional failure.

Another complexity is that the most dramatic earthquake-related liquefaction failure may occur well after the earthquake motions have ended, such as in Ojiha (1939) or Niigata (1964), Japan (Ref 4).

The influence of the degree of nonsymmetry of load application does not appear to have been addressed in any general manner, but rather the test data have been applied directly to specific cases.

Past engineering practice generally has been to design geotechnical structures to withstand earthquakes by including the equivalent static inertial forces in the traditional stability analysis and checking to see that the factor of safety is sufficiently above unity. Alternative static procedures using slip planes in the soil mass compute acceleration levels that may cause yield. Seed (Ref 8) concludes that pseudo-static analysis techniques must be used with great caution and that dynamic analysis techniques provide a more reliable basis for estimating performance and safety. The critical period of stability may occur due to redistribution of pore water pressures after the earthquake shaking has ceased. This type of failure cannot be addressed by pseudo-static analysis.

Evaluation of saturated cohesionless soils can only properly be made when pore pressures and resulting reduced confining stress and stiffness changes are taken into account. Cohesive soils also exhibit complex behavior. Thus, large deformations can occur under prolonged oscillating loads even though maximum applied stresses are less than the static strength of the soil.

Analysis of total stress does not directly yield information on pore pressures and, hence, strain softening, as the reduction in effective stress reduces shear modulus. Only a nonlinear model based upon effective stress can fully couple pore pressure generation and softening, which can significantly affect the dynamic response. Drainage of pore pressure postulated into effective stress models will be required to complete the representation of a soil.

Significant work certain to have a major impact on analysis techniques is in progress in the development of effective stress material models for use with finite element codes. The effective stress models will calculate actual dynamically induced pore pressures. Work is in progress by several researchers: Finn, Leck, and Martin (Ref 9); Ghaboussi and Dikman (Ref 10); Baladi and Rohani (Ref 11); Mroz, Norris, and Zienkiewicz (Ref 12); and Prevost and Hughes (Ref 13).

The nonlinear effective stress material models will require detailed material response data to fit the parameters required. Once an effective stress material model has been implemented in a general finite element code and verified by the engineering community, it could become the most important tool in liquefaction analysis.

FIELD INVESTIGATIONS

During the investigation of the earthquake-induced liquefaction threat at NAS North Island (Ref 14), several unusual soils were encountered. Portions of NAS originally below sea level had been reclaimed, using hydraulic fills - primarily silty sands - dredged from the bottom of San Diego Bay. These reclaimed areas had been subjected to several series of fillings, most between 1919 and 1952. As a result of investigations made on North Island in connection with foundations of existing structures, a recently filled region was selected for further study (Ref 1). Available soil data were supplemented by additional soil investigations, including dynamic split-spoon penetration tests and static cone penetrometer soundings. The split-spoon penetrations were conducted as specified in ASTM D 1586 except that a 2-1/2-inch (California-type) split spoon was used. The cone penetration soundings conformed to ASTM D 3441-75T. Based upon this information, the generalized soil profile shown in Figure 1 was developed. This soil profile encompasses an old filled bay channel, formerly known as Spanish Bight, which was hydraulically filled to its present elevation in 1945. The old bay bottom immediately prior to the first filling is represented by layer 5.

The results of split-spoon penetration tests and friction cone soundings, denoted as penetration holes P1 through P5 along the soil profile in Figure 1, are shown in Figure 2. The split-spoon penetration values near the boundary between layers 4 and 5 fall as low as one or two blows per foot, suggesting a relative density, D_r*, for soil stratum 5 of less than 50% (see Ref 14).

The relatively low friction cone penetration readings of 5 to 10 kg/sq cm shown in Figure 2 suggest values of relative density on the order of only 20% or 30%. As suggested in Reference 14, natural soils with relative densities of less than 40% are expected to be quite rare in nature. However, based upon the available information it was necessary to assume, for analysis, that the soil in the region of layer 5 could not have a relative density greater than 35%.

This type of soil appears in waterfront areas throughout California (such as at Long Beach Naval Shipyard) and, thus, is of special interest to the Navy. Most regions in California can be expected to experience ground motions of some severity relatively often (in the geologic time scale). Therefore, it was considered critical that the liquefaction potential of this soil be explored further.

---

*Relative density is a measure of the present density of a soil with respect to its maximum and minimum densities.

A program of undisturbed sampling and laboratory cyclic triaxial testing was carried out. The sampling program consisted of obtaining soil samples along the soil profile shown in Figure 1, using an Osterberg piston sampler. A description of this sampling and testing program is presented in Reference 14 and discussed elsewhere in this report.

This section of the report addresses improved reconnaissance or field liquefaction threat evaluation techniques. No matter how sophisticated and reliable analytical procedures may become, they can provide accurate response predictions only when valid input data can be obtained. In the case of minor structures, where involved analytical programs are not possible, expedient field evaluation techniques become the only available approach.

In this regard, friction cone soundings using a different type of cone were performed during April 1979 at North Island in the vicinity of P3 on the soil profile of Figure 1 (see Figure 3). This investigation used an electric friction cone rather than a mechanical cone as was used to provide the data in Figure 2. The electric cone has a standard 10-sq-cm, 60-degree tip and a 150-sq-cm sleeve, like the mechanical cone. However, rather than measuring the point and sleeve resistances over 10-cm depth increments, as with the mechanical cone, the electric cone can record penetration resistances continuously. Penetration must be interrupted only at 1-meter increments to add additional rods. A schematic picture of the electric friction cone is shown in Figure 4. A total of nine friction cone soundings was conducted. Complete results have been presented in Reference 15; however, Figure 5 shows a typical penetration resistance record. The electric cone records were found to be very similar to the mechanical cone penetration records illustrated for this area (P3 in Figure 1). Both records showed very stiff layers near depths of 3 and 16 feet and a very soft clayey (high-friction ratio) layer near a depth of 13 feet.

The liquefaction potential of a soil is directly related to its volumetric change tendencies, more specifically to its volumetric-strain/shear-strain coupling. Traditionally, the volume change properties have been the least studied from the standpoint of in situ measurements. Problems associated with sample disturbance, laboratory simulation of in situ stress state, temperature, chemical and biological environments, and soil heterogeneity, for example, severely impair any analysis based upon laboratory testing.

Thus, although in situ testing is attractive in theory, direct determination of in situ volume change properties applicable to earthquake-type loading is not yet possible. Recourse must be made to empirical correlations between volume change properties and some form of expedient field test. Various forms of penetration tests have been utilized in this regard, particularly the standard penetration test (ASTM D 1586) and the friction cone penetration test (ASTM D 3441-75T).

Unfortunately, the penetration resistance of a soil is a function not only of its volume change characteristics but also of its strength, shear stiffness, and other deformational characteristics. Penetration

resistance may be influenced by factors other than those directly influencing liquefaction potential. Therefore, it may be necessary to measure several types of response before accurate penetration test correlations become possible.

One promising device with regard to in situ volume change is a piezometer probe (Ref 16) which measures pore pressure in the tip of a penetrating cone. If, during cone penetration, positive (increased) pore water pressures are generated, then the effective stresses and, hence, the strength and resistance to penetration are reduced. Alternatively, if negative (reduced) pore water pressures occur, then the soil structure is dilating, and effective stresses are increased and so is penetration resistance. The measured incremental changes in pore pressure during penetration of saturated soils are directly related to volume change tendency. They are also a function of soil permeability and rate of penetration.

The rate at which pore water pressures reach equilibrium following cessation of penetration are direct functions of permeability. Thus, a device exists with the potential for correlation with both volume change characteristics and permeability. These two factors (along with nature of loading) are the major determinants which control the occurrence and severity of soil liquefaction.

In order to better appreciate the potential of the piezometric cone or probe for liquefaction prediction, a program of piezometric cone penetrations was intitated, through contract, at NAS North Island (Ref 15). Eight soundings were performed in the vicinity of holes P2 and P3 (see Figures 1 and 3). This work was accomplished by Fugro Gulf, Inc. of Houston, Tex., using a truck-mounted electronic cone penetrometer system. The piezometric cone is shown in Figure 6. The cone tip has the same dimensions as the standard friction cone. However, a specially designed porous element is used to allow entry of pore water. Thus, both pore pressure and total tip resistance are measured. To simplify the instrumentation, sleeve friction is not measured with this penetrometer. Pore pressure is recorded as a function of depth and penetration rate during penetration, and pore pressure dissipation is recorded as a function of time when penetration is stopped.

In operation, special precautions were required to prevent air entry (water cavitation) into the porous element during cone passage through the 5-foot-thick soil zone above the water table. These precautions included pre-drilling and casing holes to below the water table. The piezometric cone element was then saturated and encased in a water-filled membrane which maintained tip saturation while the penetrometer was being lowered in the bored hole to beneath the water table. The membrane was subsequently punctured by the advancing tip when penetration commenced into the soil at the bottom of the pre-drilled hole.

Records of the eight piezometric cone soundings are too extensive to be presented herein, but a typical data plot (probe 4A) is shown in Figure 7. A complete record is presented in Reference 15.

The pore pressures during penetration indicate both dilative (decreased pore pressure) behavior and compactive (pore pressure increase) behavior for the different in situ soil strata.

Figure 7 indicates a medium-dense layer of soil between about 6 and 10 feet deep which tends to dilate due to passage of the cone and generates a reduction in pore pressures. Beyond a depth of 10 feet, the soil strength falls off, with attendant pore pressure generation. This corresponds to the very sensitive silts (layer 5) in soil profile of Figure 1. A denser stratum is again encountered at a depth of about 15 feet (approaching layer 6) with a dramatic reduction in pore pressure generation. Tip resistance then falls off due to no further penetration.

Thus, it appears that the piezometric cone is sensitive to the type of soil response associated with liquefaction. Whether the results of such studies are precise enough to be used for reliable liquefaction potential assessments cannot be ascertained until further experience has been acquired.

LABORATORY LIQUEFACTION RESISTANCE

The most widely utilized laboratory technique for evaluating the liquefaction resistance of soils is based upon stress-controlled, cyclic triaxial testing. Liquefaction potential was measured for various candidate soil types using cyclic triaxial equipment at CEL. A description of this equipment together with representative test results for a "standard" soil has been presented in Reference 17. Reference 17 would also serve as a guide for performing cyclic triaxial testing to be used in conjunction with evaluating the seismic liquefaction potential at Naval facilities. This test equipment has been used for other CEL projects dealing with runway subgrade evaluations and resilient modular testing of airfield base course materials. Its major application, however, is for earthquake-related soil liquefaction studies, such as those conducted at NAS North Island (see Ref 1 and 14).

An in-house testing program has been initiated to investigate the liquefaction response of typical soils encountered at the waterfront and, thus, of special interest to the Navy. During the investigation outlined in Reference 14, a deposit of sensitive silty sand (layer 5 in Figure 1) was encountered which had extremely low penetration resistance. A limited number of cyclic triaxial tests on this soil were performed under contract, as outlined in Reference 1. Additional specimens acquired during this investigation were selected for further in-house cyclic triaxial testing.

The soil selected for cyclic testing was a very fine silty sand, generally dark grey in color. A typical grain size analysis is shown in Figure 8. This soil is relatively uniform with a coefficient of uniformity C_u of less than 4.0. Maximum and minimum dry densities, determined as outlined in Reference 18 were 108.2 pcf and 79.4 pcf, respectively. The density of undisturbed samples was approximately 93 pcf, which was equivalent to a relative density D_R of about 55%.

Two series of cyclic triaxial tests were performed. Series 1 consisted of seven tests performed on undisturbed tube samples 2.88 inches in diameter with a length-to-diameter ratio of approximately 2. Average dry densities varied from 90.8 to 94.2 pcf with an average density of 92.5 pcf (D_r = 53%).

Series 2 consisted of five cyclic tests on specimens 2.80 inches in diameter and 6.0 inches long. These specimens were reconstituted from the Series 1 samples by means of wet tamping.

All test specimens were consolidated isotropically under effective confining pressures of 6 to 8 psi, corresponding to the former in situ vertical effective stress value. Harmonic cyclic shear loading was applied at a frequency of 1 hertz, and the number of cycles required to reach full pore pressure ratio and 5% double amplitude strain was recorded. Pulsating deviator stress, axial strain, and pore water pressure were recorded on a Honeywell Visicorder strip-chart recorder.

The test results for Series 1 are shown in Figures 9 and 10. Also shown on Figures 9 and 10 are the best fit curves for the results of the cyclic tests reported in Reference 1 (conducted by a contractor). Test results for the Series 1 and 2 tests are compared in Figures 11 and 12.

As indicated in Figures 9 and 10, the cyclic strength curves from CEL show strengths between 30% and 45% stronger than those obtained by the contractor. Although this might be explained by the limited number of samples tested, the relative consistency or repeatability of the two separate data sources tend to preclude this. The possibility was considered that the longer period of storage of the CEL-tested samples resulted in strengths higher than the contractor's test results. This latter explanation is difficult to accept in view of the very minor differences shown between the CEL-tested undisturbed and reconstituted specimen test results shown in Figures 11 and 12. However, the results shown in Figures 11 and 12 might be influenced by specimen inhomogeneities.

For example, the reconstituted specimens formed by moist tamping would be expected to be relatively homogeneous and, therefore, provide a relatively uniform strength throughout. The undisturbed sample strengths could be influenced by small weaker zones which are the result of environmental variations during the initial sedimentation process. Such weaker zones would tend to counter the tendency of undisturbed samples to have higher strengths than reconstituted samples. Nevertheless, even though the differences between the in-house and the contractor test results could conceivably be ascribed to time-dependent structural differences, Reference 18 concludes that these differences are largely due to variations in test procedure and equipment. Thus, it appears that with these sensitive materials, carefully conducted experimental testing programs at two different facilities resulted in significant differences in liquefaction related strength measurements. A standardized procedure is essential for consistent results. References 17 and 18, prepared as part of this task, assist in this area.

EFFECTIVE STRESS SOIL MODELS

Current engineering practice does not allow for the accurate estimating of displacements of a structure founded on subsurface layers of potentially liquefiable soil. To accomplish such estimates, effective

Series 2 consisted of five cyclic tests on specimens 2.80 inches in diameter and 6.0 inches long. These specimens were reconstituted from the Series 1 samples by means of wet tamping.

All test specimens were consolidated isotropically under effective confining pressures of 6 to 8 psi, corresponding to the former in situ vertical effective stress value. Harmonic cyclic shear loading was applied at a frequency of 1 hertz, and the number of cycles required to reach full pore pressure ratio and 5% double amplitude strain was recorded. Pulsating deviator stress, axial strain, and pore water pressure were recorded on a Honeywell Visicorder strip-chart recorder.

The test results for Series 1 are shown in Figures 9 and 10. Also shown on Figures 9 and 10 are the best fit curves for the results of the cyclic tests reported in Reference 1 (conducted by a contractor). Test results for the Series 1 and 2 tests are compared in Figures 11 and 12.

As indicated in Figures 9 and 10, the cyclic strength curves from CEL show strengths between 30% and 45% stronger than those obtained by the contractor. Although this might be explained by the limited number of samples tested, the relative consistency or repeatability of the two separate data sources tend to preclude this. The possibility was considered that the longer period of storage of the CEL-tested samples resulted in strengths higher than the contractor's test results. This latter explanation is difficult to accept in view of the very minor differences shown between the CEL-tested undisturbed and reconstituted specimen test results shown in Figures 11 and 12. However, the results shown in Figures 11 and 12 might be influenced by specimen inhomogeneities.

For example, the reconstituted specimens formed by moist tamping would be expected to be relatively homogeneous and, therefore, provide a relatively uniform strength throughout. The undisturbed sample strengths could be influenced by small weaker zones which are the result of environmental variations during the initial sedimentation process. Such weaker zones would tend to counter the tendency of undisturbed samples to have higher strengths than reconstituted samples. Nevertheless, even though the differences between the in-house and the contractor test results could conceivably be ascribed to time-dependent structural differences, Reference 18 concludes that these differences are largely due to variations in test procedure and equipment. Thus, it appears that with these sensitive materials, carefully conducted experimental testing programs at two different facilities resulted in significant differences in liquefaction related strength measurements. A standardized procedure is essential for consistent results. References 17 and 18, prepared as part of this task, assist in this area.

EFFECTIVE STRESS SOIL MODELS

Current engineering practice does not allow for the accurate estimating of displacements of a structure founded on subsurface layers of potentially liquefiable soil. To accomplish such estimates, effective

stress soil models are being evaluated. Two paths are being investigated. In the first, a full nonlinear elasto-plastic model of soil skeleton behavior is desired which accounts for nonlinear behavior and volume changes with load. A second path takes a more simplified approach, separating the basic material elasto-plastic behavior and the cumulative volume change. This section will summarize results on the two approaches implemented by three soil models.

Baladi Plasticity Model

Study of an elasto-plastic cap model for cohesionless soil is being conducted at the Army Waterways Experiment Station. A minor part of the funding was provided by this work unit. A detailed description of the model and supporting equations are provided in Reference 19. The model is characterized by seven parameters which define bulk modulus variation with the first invariant of the stress tensor, shear modulus variation with second invariant plastic strain, the failure envelope, and shape of the cap. Additional parameters can be introduced for increased definition of specific soil behavior. Material properties for the model are derived from drained hydrostatic and triaxial tests. Present development is only partially complete since the model computes effective stresses, but pore pressures are not provided for. Presently, the model is set up for explicit calculation, and implicit procedures would also be desirable. Figure 13 shows typical computed undrained results, showing stress difference as a function of axial strain. Figure 13a and b shows the stress difference versus axial strain and stress pressure, respectively for a biaxial test on sand. When the soil reaches the failure envelope, it begins to fail and the loading stress difference falls as noted in Figure 13b. Figure 13c shows the stress difference-axial strain for another soil. Figure 13d shows its stress path. In this case the soil increases in strength. The characterization of the soil behavior is controlled by the material parameters input to the model.

Zienkiewicz Model

This model is a more pragmatic approach. The model consists of a simple ideally elasto-plastic model for the soil with a nonassociative flow rule corresponding to the Mohr-Coulomb surface. A separate expression for determining progressive increase in volume strain is added. The formulation is valid for undrained conditions. Data based on simple shear tests are used as the basis for developing a relationship between volume strain and a strain-related damage parameter. Additional detail may be found in Reference 20. This model is presently being implemented and evaluated.

Prevost Model

An anistropic nonlinear elasto-plastic path-dependent model for soils subject to complicated loading has been developed by Prevost. Funding was provided by CEL for implementation of this model as part of

this task. An elliptic yield surface is used in conjunction with critical state lines and an associative flow rule to compute plastic strain rate vectors. A nonassociative flow rule is then used on the yield surface. Material parameters specify the size and position of the yield surfaces with associated moduli. Table 1 and Figures 14 and 15 give results for Cook's Bayou sand. Additional information may be found in Reference 21. This model is under evaluation at the present time.

OVERVIEW

Available procedures for analyzing the liquefaction hazard to Navy facilities are inadequate. With conventional approaches to predict liquefaction at NAS North Island, factors of safety under earthquake loadings appear to vary by more than 200%. What is needed is a redefining of the liquefaction phenomenon and development of less empirical treatments.

In this regard, the loss of strength of a saturated cohesionless soil under dynamic loading can be treated under two types of response: (1) the inherently unstable situation wherein in situ shear stresses exceed undrained residual strengths, and (2) the case of accumulative displacements. In the latter case, effective stresses either are not reduced substantially during dynamic loading, or are reduced for such short durations that unrestrained failures do not occur. Nevertheless, deformations may accumulate during intervals of reduced soil stiffness and result in unacceptable levels of displacement.

It is concluded that the inherently unstable situation of the first case is unacceptable. Any situation wherein strain softening could result in residual strengths below applied stresses requires that remedial action be taken or, at least, that allowance be made for outright failure. The case of accumulation of displacements requires considerable additional effort. Unless large scale testing techniques capable of reliably modeling dynamic soil deformations throughout extended ground motion intervals are made available, the only valid avenue of approach would seem to be through effective stress soil models. Short of instrumentation and testing of prototype structures, only analytical models promise the capability of handling pore water migrations and soil structure interaction involved with the liquefaction problem.

REFERENCES

1. Civil Engineering Laboratory. Technical Note N-1555: Seismic soil liquefaction at the waterfront, by J. B. Forrest and J. M. Ferritto. Port Hueneme, Calif., May 1979.

2. __________. Technical Note N-1530: Seismic liquefaction potential, by J. M. Ferritto and J. B. Forrest. Port Hueneme, Calif., Sep 1978.

3. American Society of Civil Engineers Committee on Soil Dynamics. "Definition of terms related to liquefaction," Journal of the Geotechnical Engineering Division, ASCE, vol 104, no. GT9, Sep 1978.

4. American Society of Civil Engineers. "Liquefaction problems in geotechnical engineering," ASCE Annual Convention and Exposition, Philadelphia, Pa., Sep 27-Oct 1, 1976. (Preprint 2752)

5. G. Castro. "Comments on Seismic stability of evaluation of embankment dams; Evaluation of dam safety," American Society of Civil Engineers, Dec 1976.

6. W. D. L. Finn et al. "Cyclic pore pressures under anisotropic conditions," Earthquake Engineering and Soil Dynamics Conference, ASCE, Pasadena, Calif., Jun 1978.

7. Harvard University. Harvard Soil Mechanics, series no. 88: Liquefaction and cyclic deformation of sands; a critical review, by A. Casagrande. Cambridge, Mass., Jan 1976.

8. University of California, Earthquake Engineering Research Center. EERC Report no. 77-20: The performance of earth dams during earthquakes, by H. B. Seed, F. I. Makdisi, and P. De Alba. Berkeley, Calif., Aug 1977.

9. W. D. Finn, W. Leck, and G. R. Martin. "An effective stress model for liquefaction," Geotechnical Journal, ASCE, vol 103, no. GT6, Jun 1977.

10. University of Illinois. *UILU-ENG-77-2010: LASS II, computer* programs for analysis of seismic response and liquefaction of horizontally layered sands, by I. Ghaboussi and S. Dikmen. Urbana, Ill., Jun 1977.

11. Army Corp of Engineers, Waterways Experiment Station. Report 5-76-2: Liquefaction potential of dams and foundations development of constitutive relation for simulating the response of saturated cohesionless soil, by G. Y. Baladi and B. Nohani. Vicksburg, Miss., Aug 1978.

12. A. Mroz, V. A. Norris, and O. C. Zienkiewicz. "An isotropic hardening model for soil and its application to cyclic loading," International Journal for Numerical and Analytical Methods in Geomechanics, vol 2, 1978.

13. J. H. Prevost, and T. J. R. Hughes. "Mathematical modeling of cyclic soil behavior," Earthquake Engineering and Soil Dynamics, ASCE, vol 11, 1978.

14. Civil Engineering Laboratory. Technical Report R-847: An earthquake analysis of the liquefaction potential at the Naval Air Station North Island, by J. B. Forrest and J. M. Ferritto. Port Hueneme, Calif., Sep 1976.

15. __________. Project no. 79-023: Piezometric cone penetrometer soundings, North Island Naval Air Station. Houston, Tex., Fugro Gulf, Inc., Jun 1979.

16. A. E. Z. Wissa, R. T. Martin, and J. E. Garlanger. "The Piezometer probe," in Proceedings of the Conference on In Situ Measurement of Soil Properties, Vol I, North Carolina State University, Raleigh, N.C., 1-4 Jun 1975. New York, N.Y., American Society of Civil Engineers, 1975.

17. Civil Engineering Laboratory. Technical Memorandum (in publication): Cyclic triaxial test procedure for dynamic soil strengths, by G. Wu. Port Hueneme, Calif.

18. __________. Technical Memorandum (in publication): Cyclic strength of NAS North Island Soil, by G. Wu. Port Hueneme, Calif.

19. G. Y. Baladi. Lecture series on the cap-type constitutive model, presented at the Civil Engineering Laboratory, Port Hueneme, Calif., 20-23 Nov 1978.

20. O. C. Zienkiewicz, C. T. Chang, and E. Henton. "Nonlinear seismic response and liquefaction," International Journal for Numerical Methods in Geomechanics, vol 2, Jul 1978, pp 381-404.

21. J. A. Prevost. Mathematical modeling of soil stress-strain strength behavior. (unpublished paper)

Table 1. Model Parameters for Cook's Bayou Sand (σ'_{vc} = 50 psi) (Ref 21)

($G = 400\ \sigma'_{vc}$, $B_1 = 470.6\ \sigma'_{vc}$, $n = 0.5$)

m	Model Parameters				
	$\beta^{(m)}/\sigma'_{vc}$	$k^{(m)}/\sigma'_{vc}$	h_m/σ'_{vc}	B'_m/σ'_{vc}	A_m/σ'_{vc}
2	0.800	0.424	800.00	-12,325.089	0.080
3	0.700	0.636	800.000	-8,333.974	0.080
4	0.600	0.849	800.000	-2,000.000	0.080
5	0.550	0.955	800.000	-2,000.000	0.080
6	0.500	1.061	800.000	-2,000.000	0.080
7	0.633	1.344	371.429	-2,000.000	0.059
8	0.750	1.591	270.011	-2,000.000	0.040
9	0.882	1.871	218.370	-2,000.000	0.029
10	1.025	2.174	204.684	-2,000.000	0.024
11	1.138	2.415	177.342	-2,000.000	0.022
12	1.256	2.663	162.053	-2,000.000	0.020
13	1.316	2.791	122.269	-2,000.000	0.019
14	1.376	2.920	102.628	-2,000.000	0.018
15	1.500	3.182	72.687	-2,000.000	0.017
16	1.626	3.450	49.335	-2,000.000	0.014
17	1.755	3.722	47.909	-2,000.000	0.014
18	1.819	3.860	27.486	-2,000.000	0.014
19	1.885	3.998	16.148	-2,000.000	0.014
20	4.000	20.000	0.000	-2,000.000	0.014

SYMBOLS:

D_r = Relative density, present desnity as compared to maximum and minimum density states

h_m = Plastic shear modulus associated with yield surface m

$k^{(m)}$ = Size of yield surface m

m = Number representing a particular rested yield surface

n = Measured soil parameter

p = Pressure

A_m = Soil parameter

B_m = Plastic bulk modulus associated with yield surface m

Table 1. Continued

SYMBOLS: (cont'd)	G	=	Elastic shear modulus
	β	=	Coordinate locating center of yield surface
	σ'_{vc}	=	Effective confining stress
	σ_{3c}	=	Chamber confining pressure in triaxial test
	σ_{dp}	=	Deviator stress in triaxial test (dynamic)
	k_c	=	Ratio of horizontal to vertical stress in triaxial test
	E_v	=	Volumetric strain
	σ_v,σ_y	=	Stresses in coordinate directions x,y

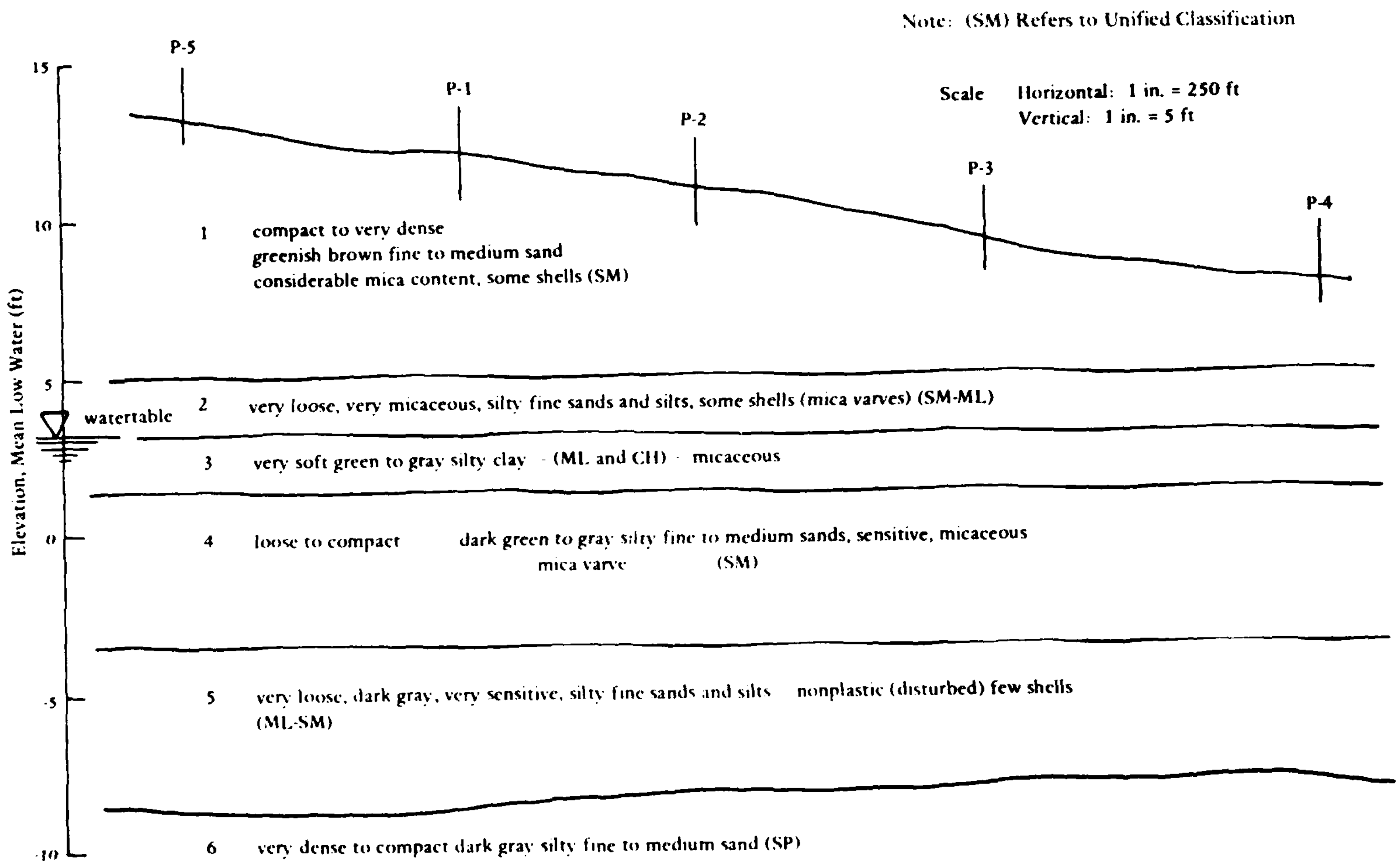

Figure 1. Generalized soil profile across former Spanish Bight. (Ref 14).

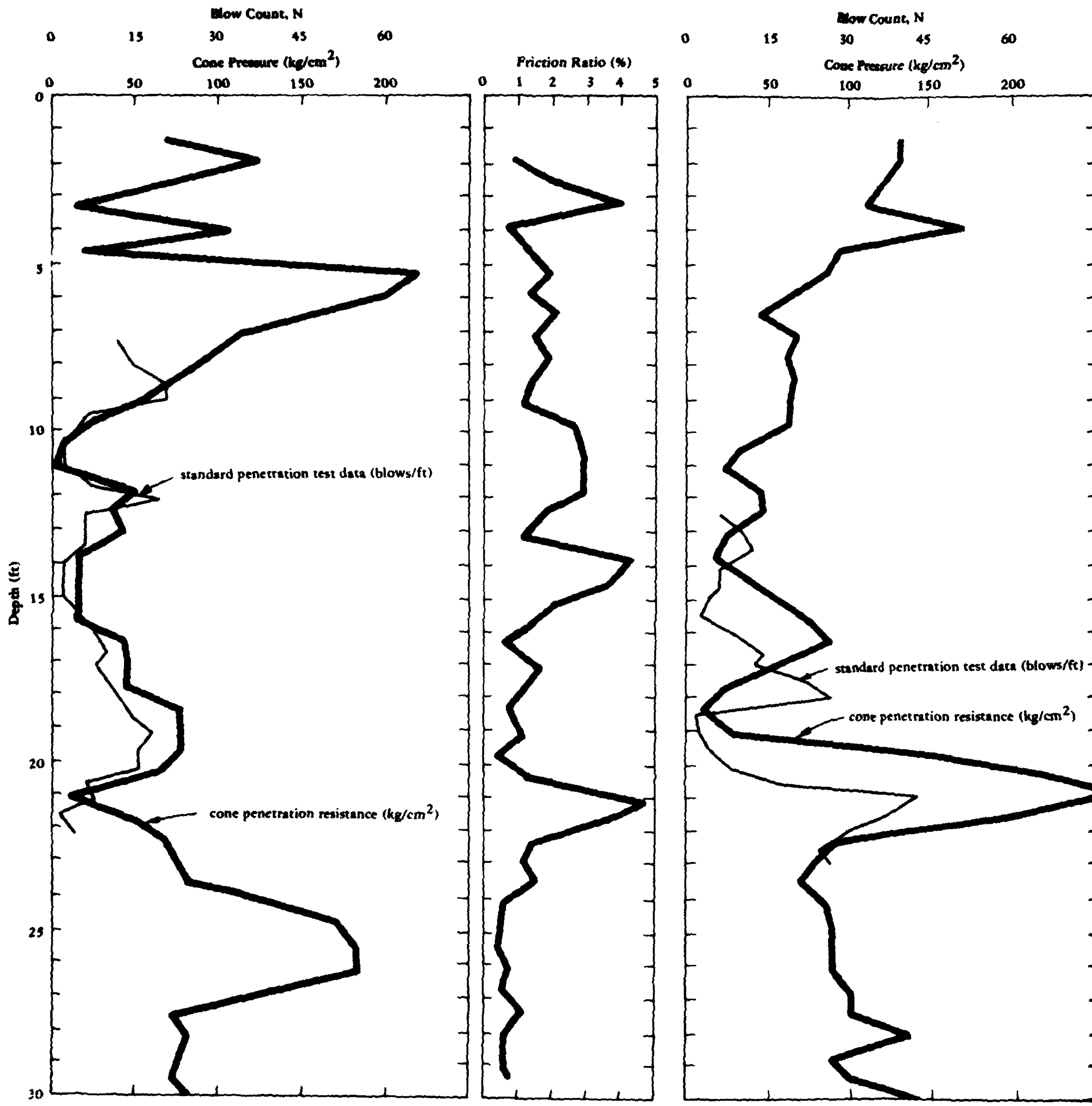

Penetration Hole No. P-5

Penetration Hole No. P-1

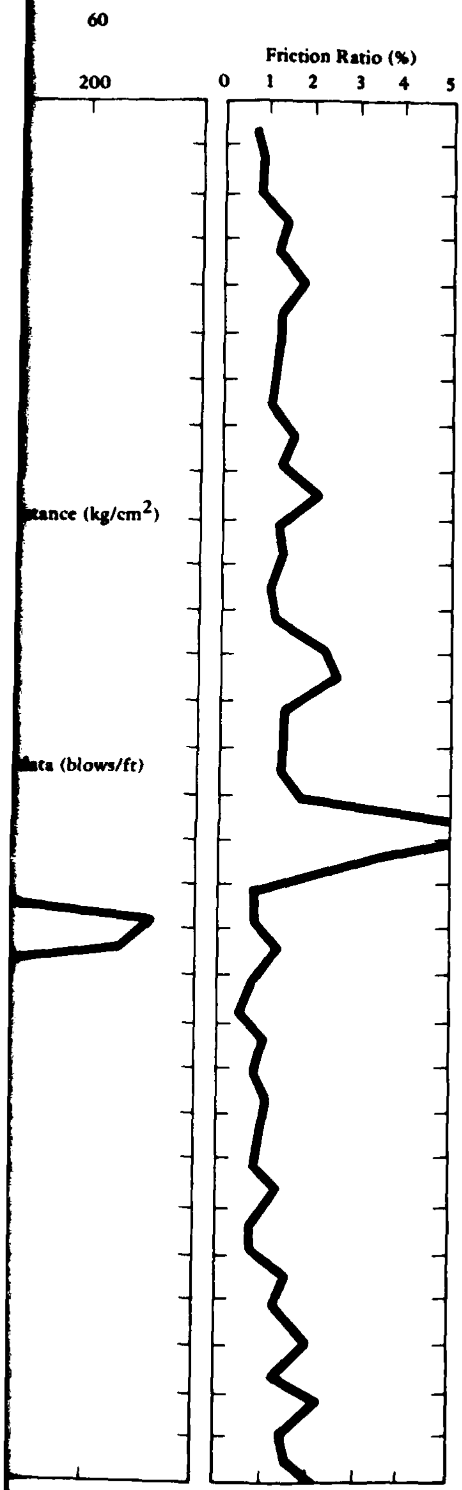

Hole No. P-2

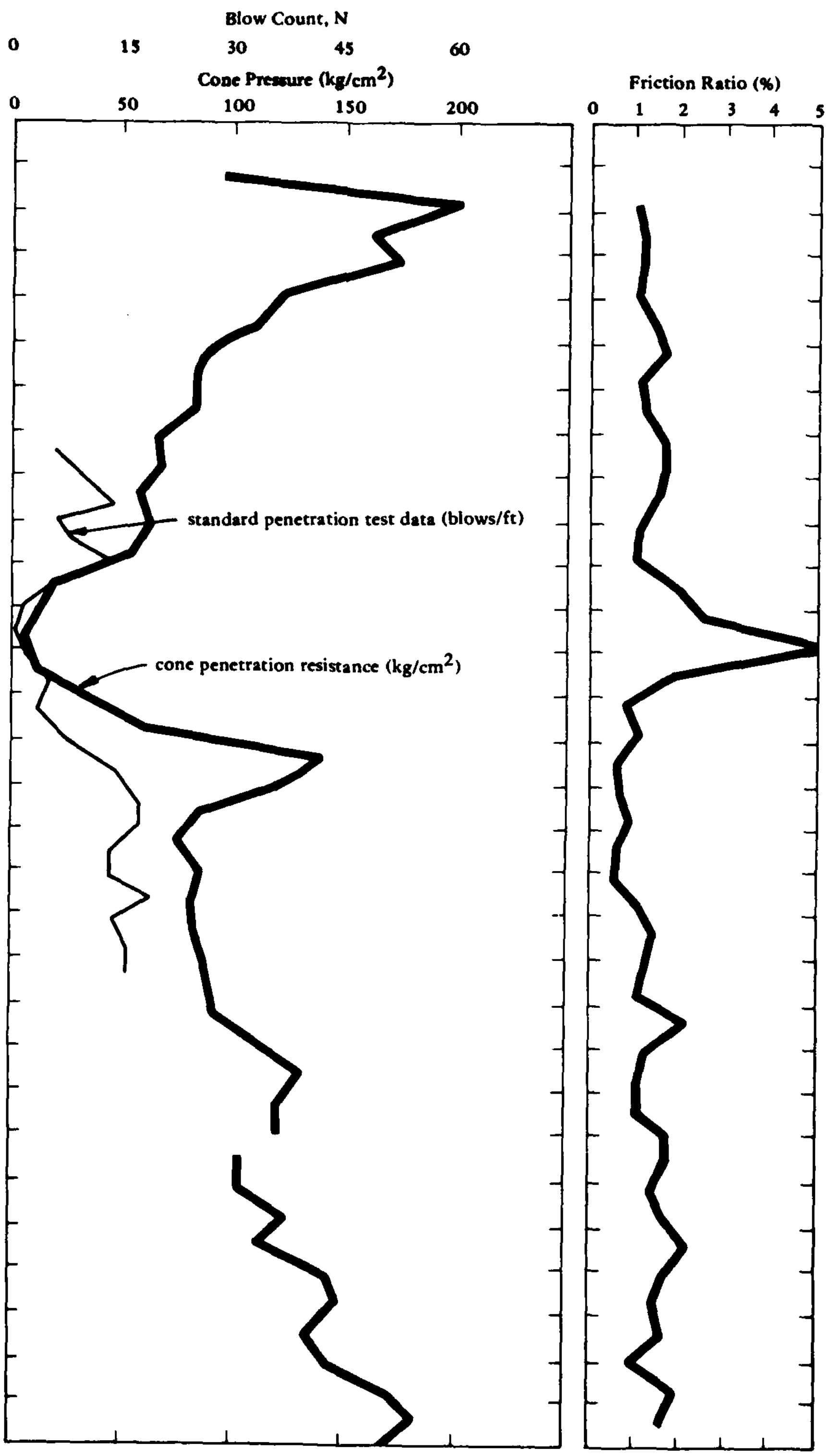

Penetration Hole No. P-3

f 14).

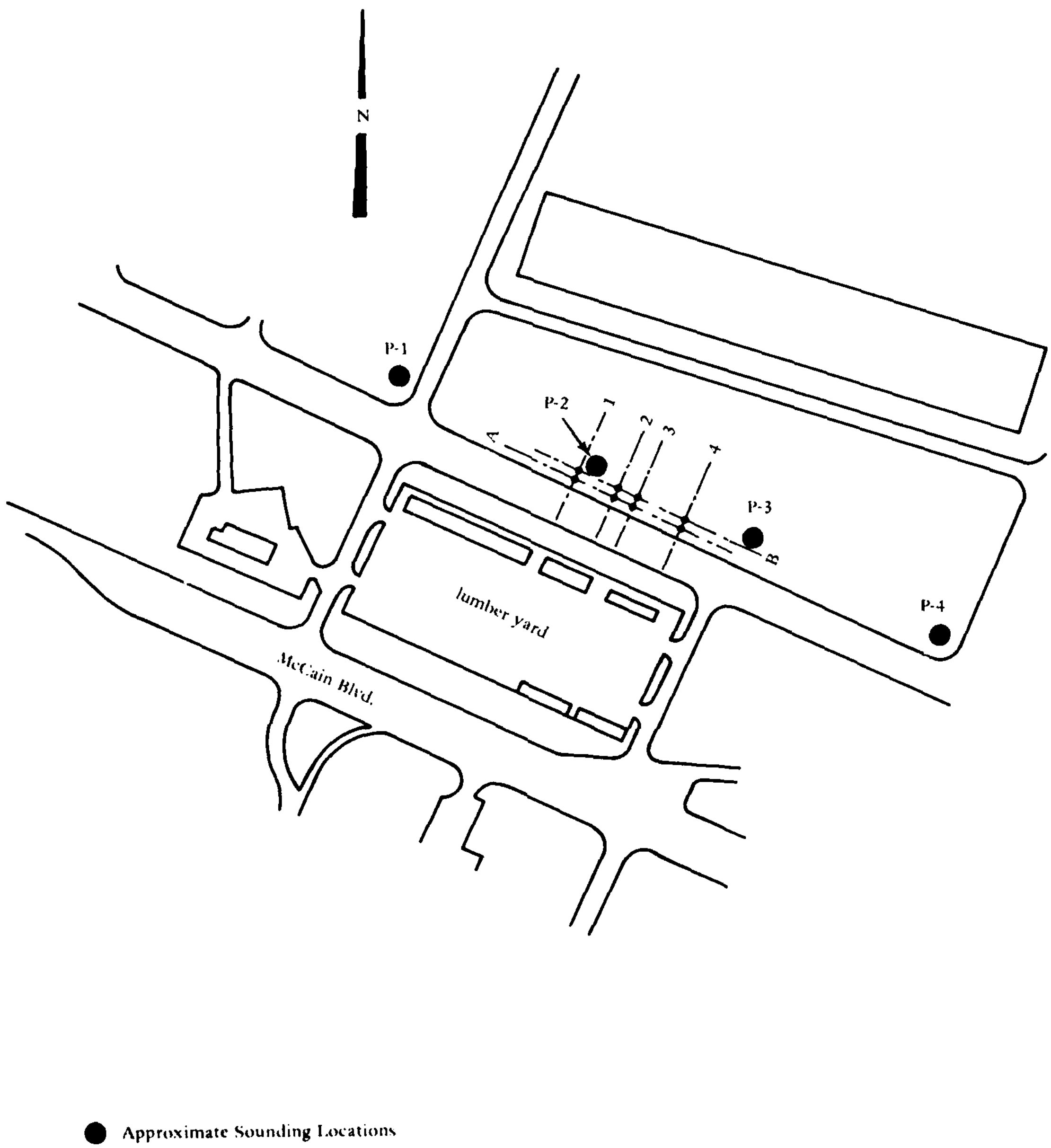

Figure 3. Cone penetrometer sounding plan, NAS, North Island, San Diego, Calif. (Ref 15).

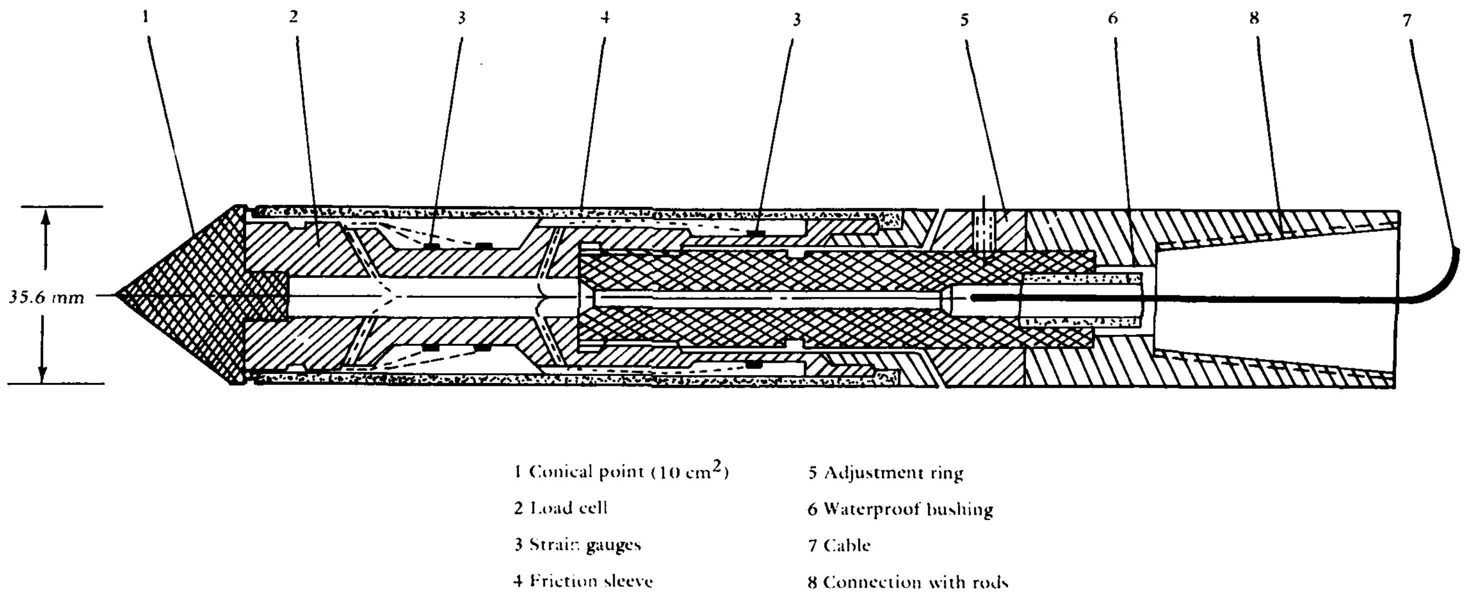

Figure 4. Cross-section of friction cone penetrometer. (Ref 15).

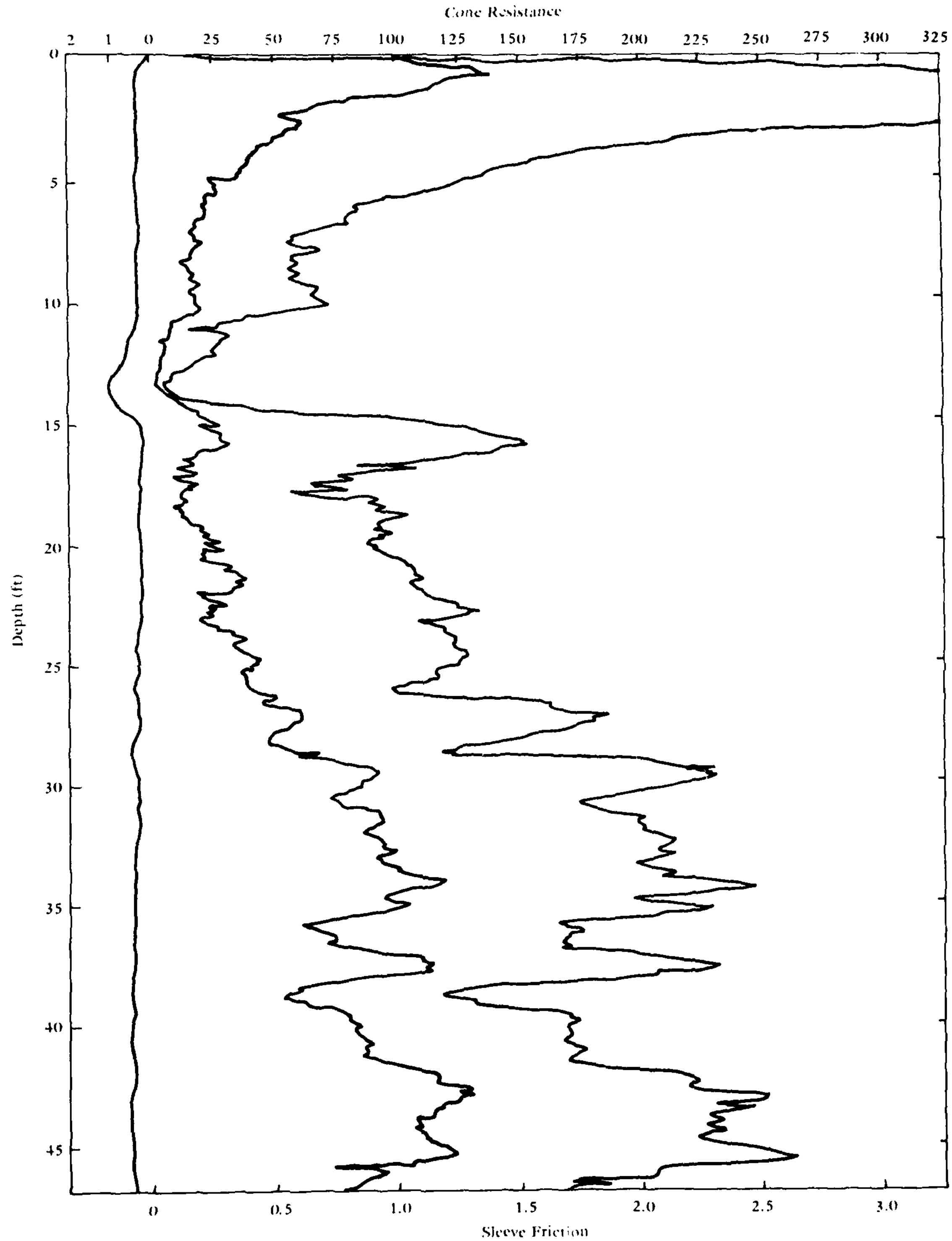

Figure 5. Cone penetration test no. 3A.

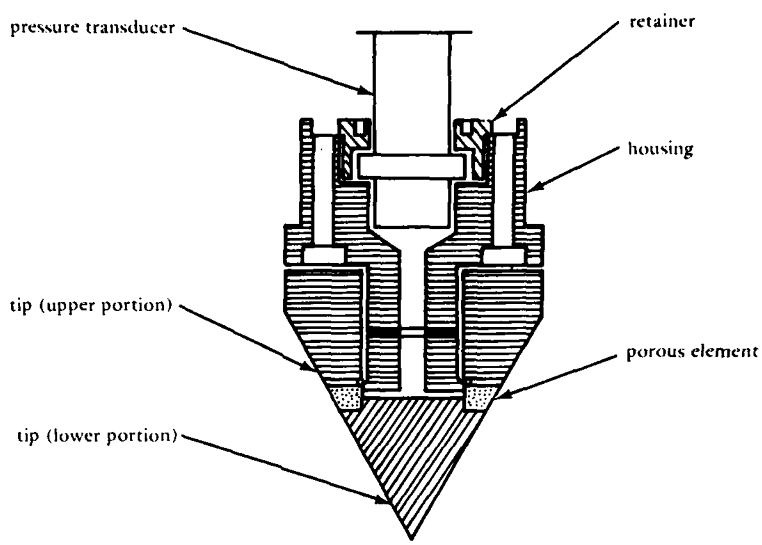

Figure 6. Pore pressure cone tip assembly. (Ref 15).

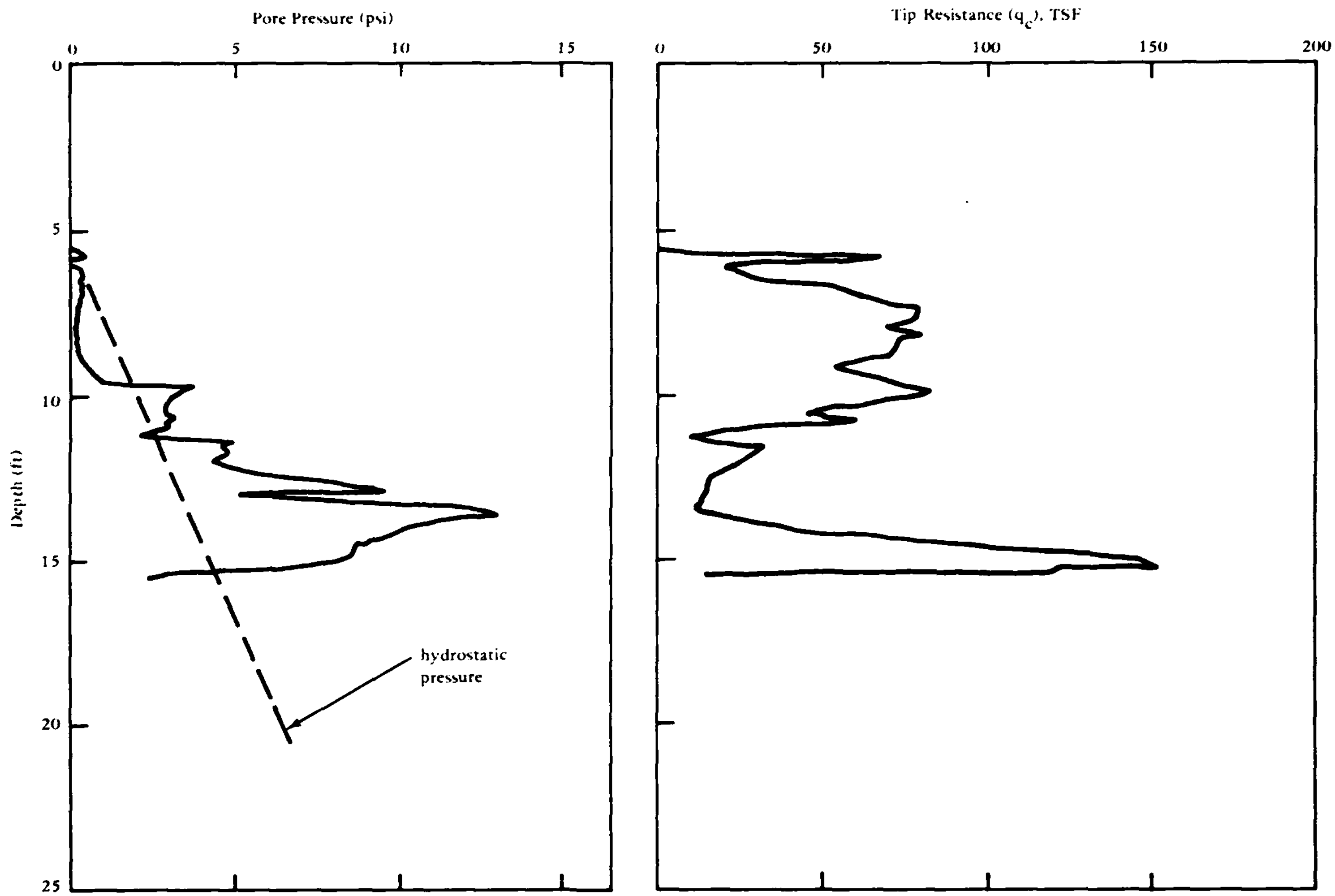

Figure 7. Piezometer sounding.

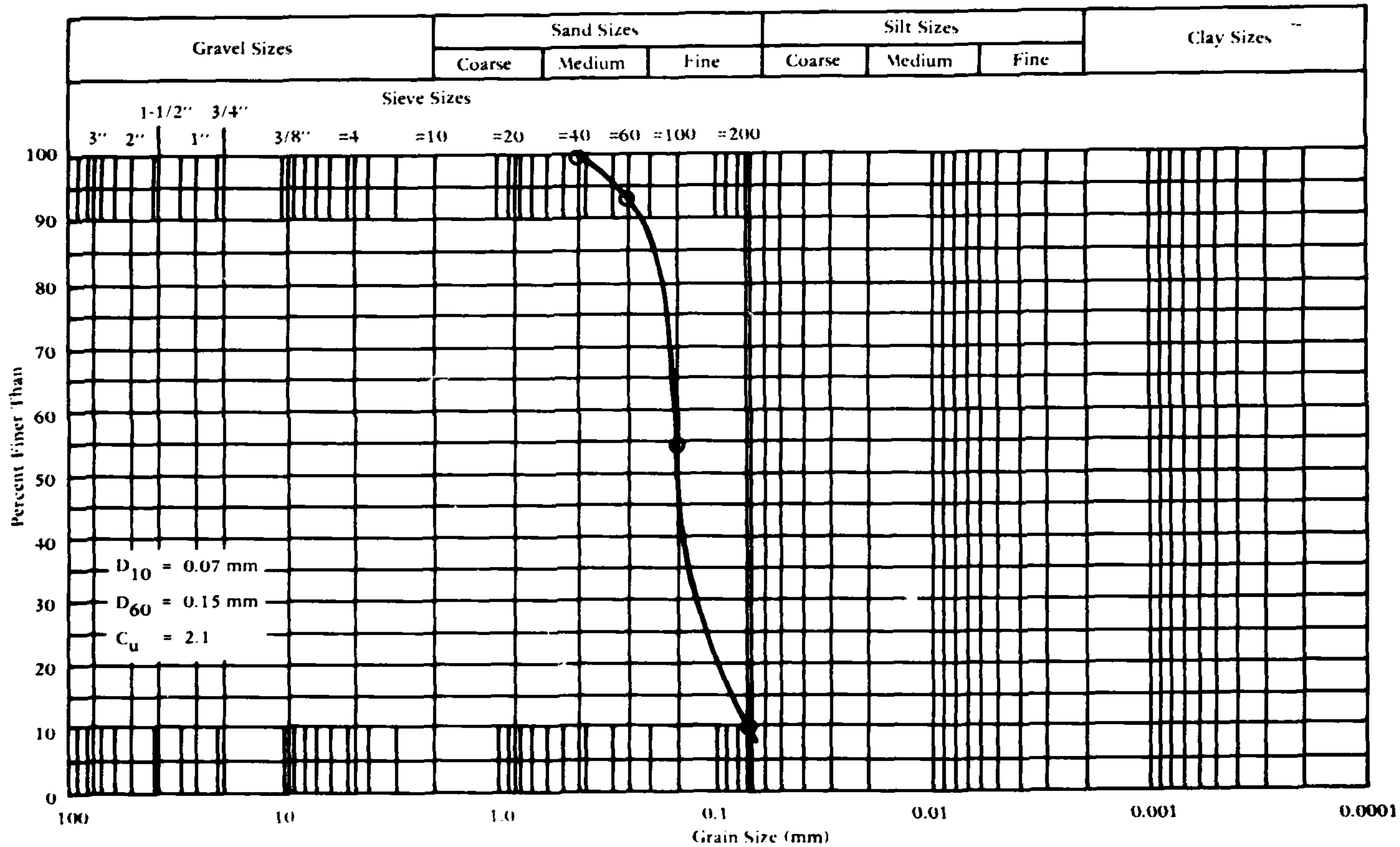

Note: M.I.T. Grain Size Scale.

Figure 8. Typical grain size distribution curve for NAS, North Island soil. (Ref 18).

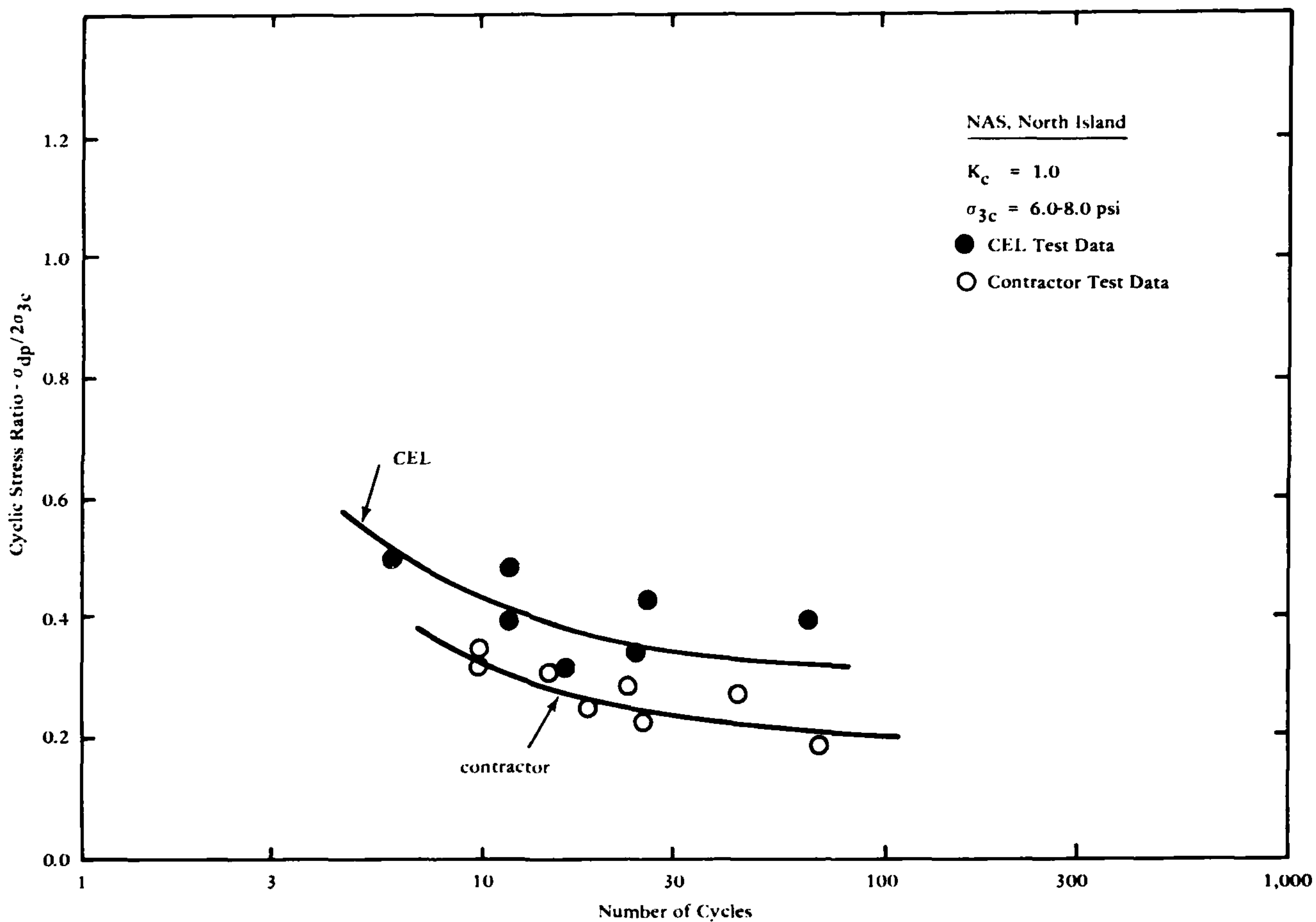

Figure 9. Comparison of cyclic triaxial data on undisturbed field samples at initial liquefaction between CEL and the contractor. (Ref 18).

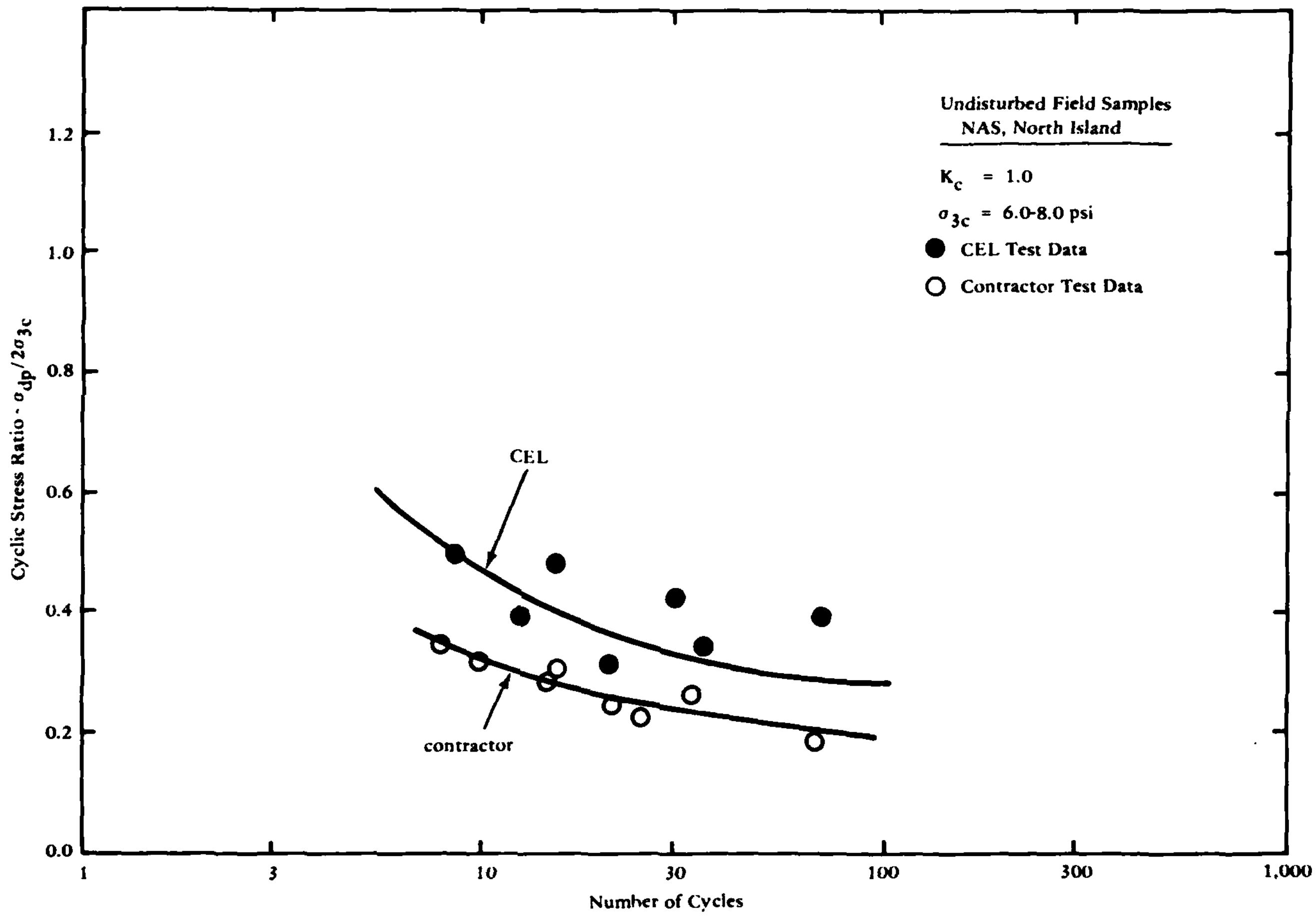

Figure 10. Comparison of cyclic triaxial data at 5% double amplitude strain between CEL and the contractor. (Ref 18).

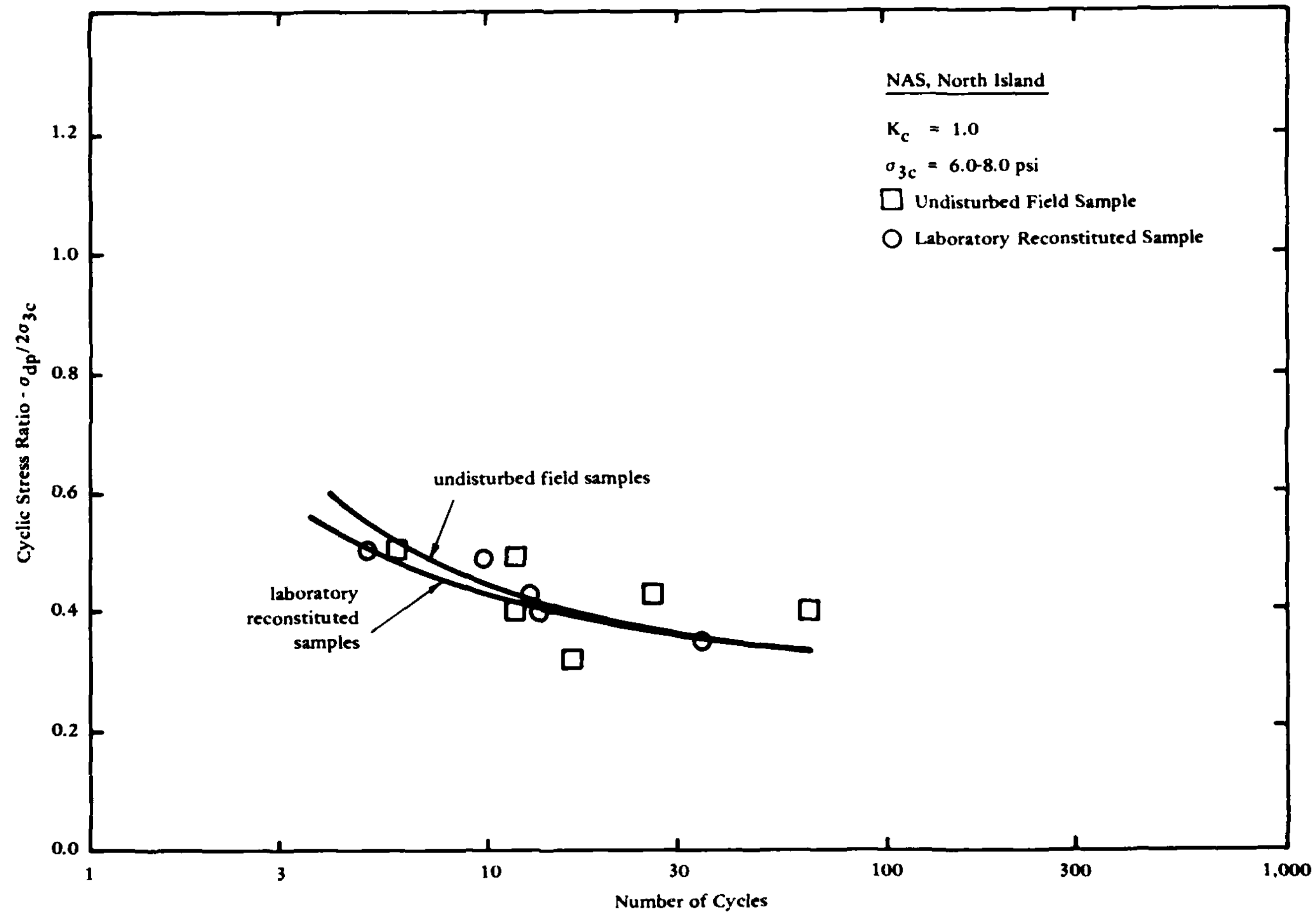

Figure 11. Comparison of cyclic strength between undisturbed field samples and laboratory reconstituted samples at initial liquefaction. (Ref 18).

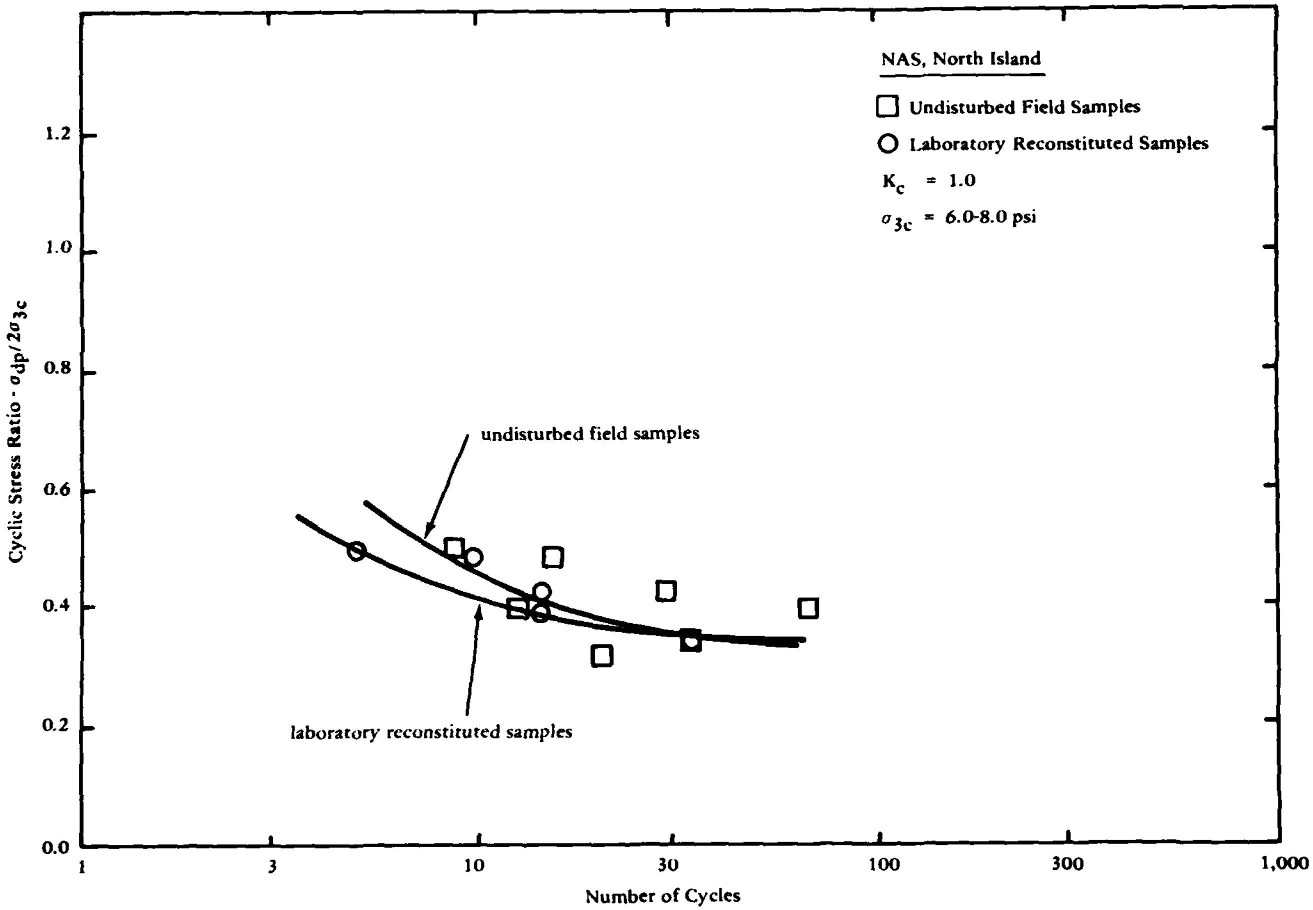

Figure 12. Comparison of cyclic strength between undisturbed field samples and laboratory reconstituted samples at 5% double amplitude strain. (Ref 18).

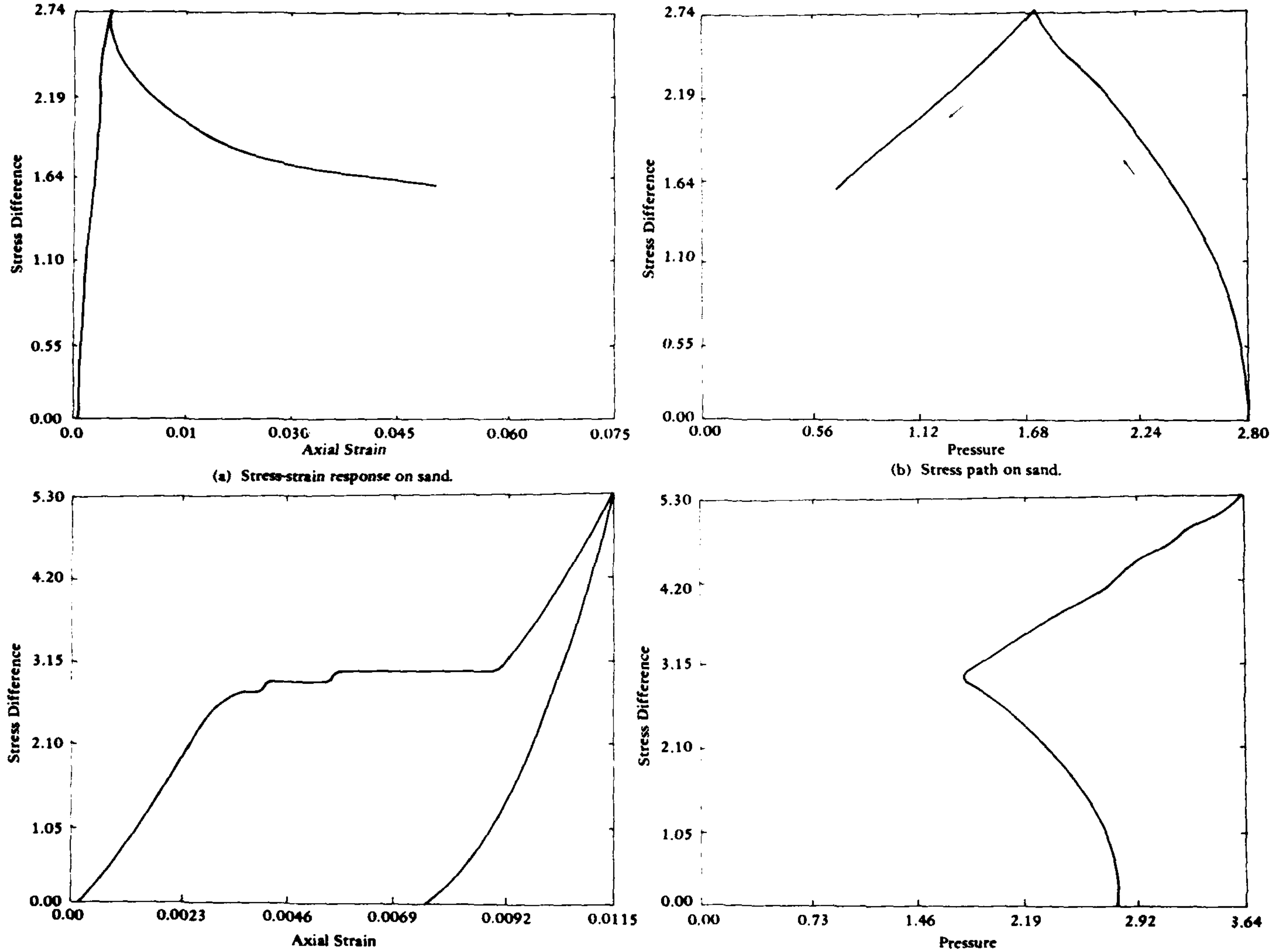

(a) Stress-strain response on sand.

(b) Stress path on sand.

(c) Stress-strain response on dense sand.

(d) Stress path on dense sand.

Figure 13. Simulated undrained triaxial tests.

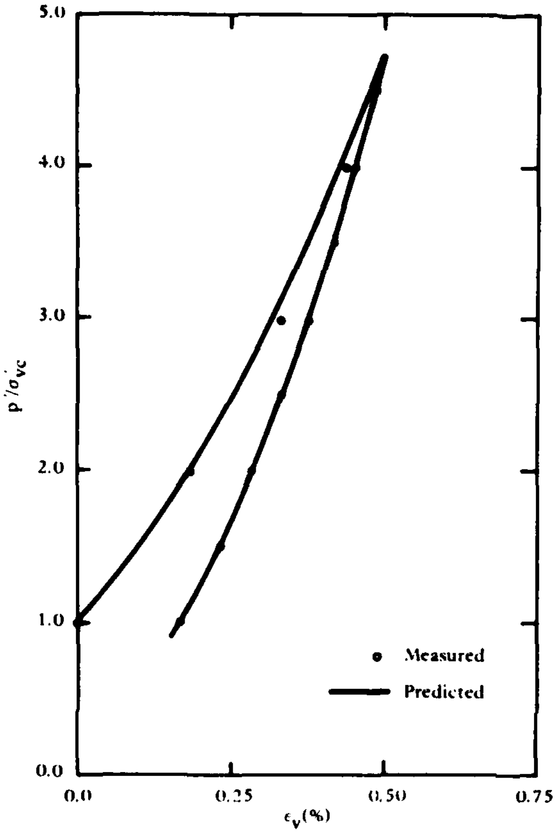

Figure 14. Calculated and measured stress-strain behavior for consolidation/swelling tests with Cook's Bayou Sand. (Ref 21).

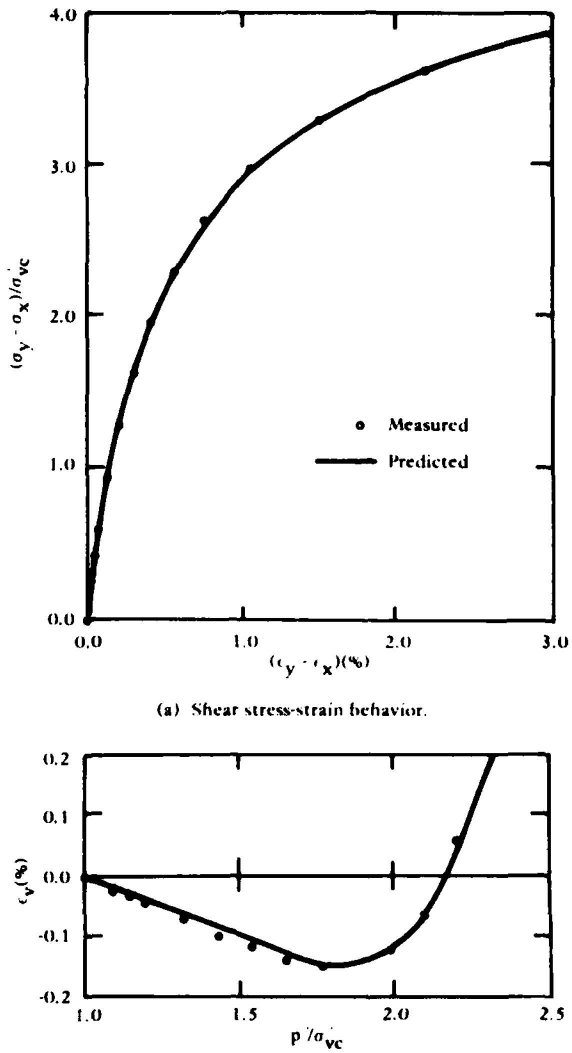

(a) Shear stress-strain behavior.

(b) Volumetric stress-strain behavior.

Figure 15. Calculated and measured stress-strain behavior for triaxial soil test with Cook's Bayou Sand. (Ref 21).

DISTRIBUTION LIST

AF HQ PREES Washington DC (R P Reid)
AFB AF Tech Office (Mgt & Ops), Tyndall, FL; AFCEC/XR,Tyndall FL; CESCH, Wright-Patterson; HQAFESC/DEMM, Tyndall AFB, FL; MAC/DET (Col. P. Thompson) Scott, IL; SAMSO/MNND, Norton AFB CA; Stinfo Library, Offutt NE
ARCTICSUBLAB Code 54, San Diego, CA
ARMY BMDSC-RE (H. McClellan) Huntsville AL; DAEN-MPE-D Washington DC; Tech. Ref. Div., Fort Huachuca, AZ
ARMY COASTAL ENGR RSCH CEN Fort Belvoir VA; R. Jachowski, Fort Belvoir VA
ARMY COE Philadelphia Dist. (LIBRARY) Philadelphia, PA
ARMY CORPS OF ENGINEERS MRD-Eng. Div., Omaha NE; Seattle Dist. Library, Seattle WA
ARMY ENG DIV HNDED-CS, Huntsville AL; HNDED-SR, Huntsville, AL
ARMY ENG WATERWAYS EXP STA Library, Vicksburg MS
ARMY ENGR DIST. Library, Portland OR
ARMY ENVIRON. HYGIENE AGCY Water Qual Div (Doner), Aberdeen Prov Ground, MD
ARMY MATERIALS & MECHANICS RESEARCH CENTER Dr. Lenoe, Watertown MA
ARMY MOBIL EQUIP R&D COM Mr. Cevasco, Fort Belvoir MD
ASST SECRETARY OF THE NAVY Spec. Assist Energy (Leonard), Washington, DC
CINCLANT Civil Engr. Supp. Plans. Ofr Norfolk, VA
CNO Code NOP-964, Washington DC; OP987J (J. Boosman), Pentagon
COMOCEANSYSPAC SCE, Pearl Harbor HI
DEFENSE DOCUMENTATION CTR Alexandria, VA
DEFENSE INTELLIGENCE AGENCY Dir., Washington DC
DNA STTL, Washington DC
DOD Explosives Safety Board (Library), Washington DC
FLTCOMBATTRACENLANT PWO, Virginia Bch VA
MARINE CORPS BASE M & R Division, Camp Lejeune NC; PWO Camp Lejeune NC; PWO, Camp S. D. Butler, Kawasaki Japan
MARINE CORPS HQS Code LFF-2, Washington DC
MCAS Facil. Engr. Div. Cherry Point NC; Code PWE, Kaneohe Bay HI; Code S4, Quantico VA; PWO Kaneohe Bay HI
MCDEC P&S Div Quantico VA
MCLSBPAC B520, Barstow CA
MCRD PWO, San Diego Ca
NAD Engr. Dir. Hawthorne, NV
NAF PWO Sigonella Sicily; PWO, Atsugi Japan
NAS CO, Guantanamo Bay Cuba; Code 114, Alameda CA; Code 183 (Fac. Plan BR MGR); Code 187, Jacksonville FL; Code 18700, Brunswick ME; Code 70, Atlanta, Marietta GA; Dir. Util. Div., Bermuda; ENS Buchholz, Pensacola, FL; Lead. Chief. Petty Offr. PW/Self Help Div, Beeville TX; PW (J. Maguire), Corpus Christi TX; PWD Maint. Div., New Orleans, Belle Chasse LA; PWD, Willow Grove PA; PWO Belle Chasse, LA; PWO Chase Field Beeville, TX; PWO Key West FL; PWO, Dallas TX; PWO, Glenview IL; SCE Lant Fleet Norfolk, VA; SCE Norfolk, VA; SCE, Barbers Point HI; Security Offr, Alameda CA
NATL RESEARCH COUNCIL Naval Studies Board, Washington DC
NAVACT PWO, London UK
NAVAEROSPREGMEDCEN SCE, Pensacola FL
NAVCOASTSYSTCTR Code 423 (D. Good), Panama City FL; Library Panama City, FL
NAVCOMMAREAMSTRSTA PWO, Norfolk VA; PWO, Wahiawa HI; SCE Unit 1 Naples Italy
NAVCOMMSTA Code 401 Nea Makri, Greece; PWO, Exmouth, Australia
NAVEDTRAPRODEVCEN Tech. Library
NAVEDUTRACEN Engr Dept (Code 42) Newport, RI
NAVFAC PWO, Brawdy Wales UK; PWO, Cape Hatteras, Buxton NC
NAVFACENGCOM Code 043 Alexandria, VA; Code 044 Alexandria, VA; Code 0451 Alexandria, VA; Code 0453 (D. Potter) Alexandria, VA; Code 0454B Alexandria, Va; Code 04B5 Alexandria, VA; Code 100 Alexandria, VA; Code 1002B (J. Leimanis) Alexandria, VA; Code 1113 (T. Stevens) Alexandria, VA; Morrison Yap, Caroline Is.; P W Brewer Alexandria, VA
NAVFACENGCOM - CHES DIV. Code 101 Wash. DC; Code 405 Wash. DC; Code FPO-1 Wash. DC; FPO-1

(Spencer) Wash, DC; Code 402 (D Scheesele) Washington, DC
NAVFACENGCOM - LANT DIV. Eur. BR Deputy Dir, Naples Italy; European Branch, New York; RDT&ELO 102, Norfolk VA
NAVFACENGCOM - NORTH DIV. (Boretsky) Philadelphia, PA; Code 09P (LCDR A.J. Stewart); Code 1028, RDT&ELO, Philadelphia PA; Design Div. (R. Masino), Philadelphia PA; ROICC, Contracts, Crane IN
NAVFACENGCOM - PAC DIV. (Kyi) Code 101, Pearl Harbor, HI; Code 2011 Pearl Harbor, HI; Code 402, RDT&E, Pearl Harbor HI; Commander, Pearl Harbor, HI
NAVFACENGCOM - SOUTH DIV. Code 90, RDT&ELO, Charleston SC
NAVFACENGCOM - WEST DIV. Code 04B San Bruno, CA; RDT&ELO Code 2011 San Bruno, CA
NAVFACENGCOM CONTRACT AROICC, Point Mugu CA; Eng Div dir, Southwest Pac, Manila, PI; OICC, Southwest Pac, Manila, PI; OICC/ROICC, Balboa Canal Zone; ROICC LANT DIV., Norfolk VA; ROICC, Diego Garcia Island; ROICC, Keflavik, Iceland
NAVHOSP LT R. Elsbernd, Puerto Rico
NAVMAG SCE, Guam
NAVOCEANSYSCEN Code 5311 San Diego, CA
NAVPETOFF Code 30, Alexandria VA
NAVPGSCOL Code 61WL (O. Wilson) Monterey CA
NAVPHIBASE CO, ACB 2 Norfolk, VA; Code S3T, Norfolk VA
NAVREGMEDCEN Code 29, Env. Health Serv. (Al Bryson) San Diego, CA; SCE (D. Kaye); SCE, Camp Pendleton CA; SCE, Oakland CA
NAVSCOLCECOFF C35 Port Hueneme, CA; CO, Code C44A Port Hueneme, CA
NAVSEASYSCOM Code OOC (LT R. MacDougal), Washington DC
NAVSECGRUACT PWO, Adak AK; PWO, Torri Sta, Okinawa
NAVSHIPYD Code 404 (LT J. Riccio), Norfolk, Portsmouth VA; Code 410, Mare Is., Vallejo CA; Code 440 Portsmouth NH; Code 440, Norfolk; Code 440, Puget Sound, Bremerton WA; L.D. Vivian; PWO, Mare Is.; Tech Library, Vallejo, CA
NAVSTA CO Naval Station, Mayport FL; CO Roosevelt Roads P.R. Puerto Rico; Engr. Dir., Rota Spain; Long Beach, CA; Maint. Div. Dir/Code 531, Rodman Canal Zone; PWD (LTJG.P.M. Motolenich), Puerto Rico; PWO Midway Island; PWO, Keflavik Iceland; PWO, Mayport FL; ROICC, Rota Spain; SCE, Guam; SCE, San Diego CA; SCE, Subic Bay, R.P.; Utilities Engr Off. (A.S. Ritchie), Rota Spain
NAVSUPPACT CO, Seattle WA; Code 413, Seattle WA; LTJG McGarrah, SEC, Vallejo, CA
NAVSURFWPNCEN PWO, White Oak, Silver Spring, MD
NAVTECHTRACEN SCE, Pensacola FL
NAVWPNCEN Code 2636 (W. Bonner), China Lake CA; PWO (Code 26), China Lake CA; ROICC (Code 702), China Lake CA
NAVWPNSTA PW Office (Code 09C1) Yorktown, VA
NAVWPNSUPPCEN Code 09 Crane IN
NCBU 405 OIC, San Diego, CA
PWC Code 420, Pensacola, FL
NCBC CEL AOIC Port Hueneme CA; Code 155, Port Hueneme CA; Code 156, Port Hueneme, CA; PW Engrg, Gulfport MS
NCBU 411 OIC, Norfolk VA
NCR 20, Commander
NMCB 5, Operations Dept.; Forty, CO; THREE, Operations Off.
NORDA Code 440 (Ocean Rsch Off) Bay St. Louis MS
NRL Code 8400 Washington, DC; Code 8441 (R.A. Skop), Washington DC; Rosenthal, Code 8440, Wash. DC
NSD SCE, Subic Bay, R.P.
NUSC Code 131 New London, CT; Code EA123 (R.S. Munn), New London CT
ONR Code 700F Arlington VA; Dr. A. Laufer, Pasadena CA
PHIBCB 1 P&E, Coronado, CA
PMTC Pat. Counsel, Point Mugu CA
PWC ACE Office (LTJG St. Germain) Norfolk VA; CO Norfolk, VA; CO, (Code 10), Oakland, CA; CO, Great Lakes IL; Code 10, Great Lakes, IL; Code 120, Oakland CA; Code 120C, (Library) San Diego, CA; Code 128, Guam; Code 154, Great Lakes, IL; Code 200, Great Lakes IL; Code 220 Oakland, CA; Code 220.1, Norfolk VA; Code 30C, San Diego, CA; Code 400, Great Lakes, IL; Code 400, Oakland, CA; Code 400, Pearl Harbor, HI; Code 400, San Diego, CA; Code 420, Great Lakes, IL; Code 420, Oakland, CA; Code 610, San Diego Ca; Library, Subic Bay, R.P.; Utilities Officer, Guam; XO (Code 20) Oakland, CA
SPCC PWO (Code 120) Mechanicsburg PA

UCT TWO OIC, Norfolk, VA
U.S. MERCHANT MARINE ACADEMY Kings Point, NY (Reprint Custodian)
US DEPT OF INTERIOR Bureau of Land MNGMNT - Code 733 (T.E. Sullivan) Wash, DC
US GEOLOGICAL SURVEY Off. Marine Geology, Piteleki, Reston VA
USCG G-EOE-4/61 (T. Dowd), Washington DC
USCG R&D CENTER D. Motherway, Groton CT
USNA Ocean Sys. Eng Dept (Dr. Monney) Annapolis, MD; Oceanography Dept (Hoffman) Annapolis MD; PWD Engr. Div. (C. Bradford) Annapolis MD
CALIF. DEPT OF NAVIGATION & OCEAN DEV. Sacramento, CA (G. Armstrong)
CALIFORNIA STATE UNIVERSITY LONG BEACH, CA (CHELAPATI); LONG BEACH, CA (YEN)
COLORADO STATE UNIV., FOOTHILL CAMPUS Fort Collins (Nelson)
CORNELL UNIVERSITY Ithaca NY (Serials Dept, Engr Lib.)
DAMES & MOORE LIBRARY LOS ANGELES, CA
DUKE UNIV MEDICAL CENTER B. Muga, Durham NC; DURHAM, NC (VESIC)
FLORIDA ATLANTIC UNIVERSITY Boca Raton FL (Ocean Engr Dept., C. Lin); Boca Raton FL (W. Tessin); Boca Raton, FL (McAllister)
FLORIDA TECHNOLOGICAL UNIVERSITY ORLANDO, FL (HARTMAN)
GEORGIA INSTITUTE OF TECHNOLOGY Atlanta GA (B. Mazanti)
IOWA STATE UNIVERSITY Ames IA (CE Dept, Handy)
LEHIGH UNIVERSITY BETHLEHEM, PA (MARINE GEOTECHNICAL LAB., RICHARDS); Bethlehem PA (Fritz Engr. Lab No. 13, Beedle); Bethlehem PA (Linderman Lib. No.30, Flecksteiner)
LIBRARY OF CONGRESS WASHINGTON, DC (SCIENCES & TECH DIV)
MICHIGAN TECHNOLOGICAL UNIVERSITY Houghton, MI (Haas)
MIT Cambridge MA; Cambridge MA (Rm 10-500, Tech. Reports, Engr. Lib.); Cambridge MA (Whitman)
NORTHWESTERN UNIV Z.P. Bazant Evanston IL
NY CITY COMMUNITY COLLEGE BROOKLYN, NY (LIBRARY)
OREGON STATE UNIVERSITY (CE Dept Grace) Corvallis, OR; CORVALLIS, OR (CE DEPT, BELL); Corvalis OR (School of Oceanography)
PENNSYLVANIA STATE UNIVERSITY UNIVERSITY PARK, PA (GOTOLSKI)
PURDUE UNIVERSITY Lafayette IN (Leonards); Lafayette, IN (Altschaeffl); Lafayette, IN (CE Engr. Lib)
SAN DIEGO STATE UNIV. I. Noorany San Diego, CA; Dr. Krishnamoorthy, San Diego CA
SEATTLE U Prof Schwaegler Seattle WA
STANFORD UNIVERSITY Engr Lib, Stanford CA
TEXAS A&M UNIVERSITY College Station TX (CE Dept. Herbich); W.B. Ledbetter College Station, TX
UNIVERSITY OF CALIFORNIA BERKELEY, CA (CE DEPT, MITCHELL); DAVIS, CA (CE DEPT, TAYLOR); LIVERMORE, CA (LAWRENCE LIVERMORE LAB, TOKARZ); La Jolla CA (Acq. Dept, Lib. C-075A); M. Duncan, Berkeley CA; SAN DIEGO, CA, LA JOLLA, CA (SEROCKI)
UNIVERSITY OF DELAWARE Newark, DE (Dept of Civil Engineering, Chesson)
UNIVERSITY OF HAWAII HONOLULU, HI (SCIENCE AND TECH. DIV.)
UNIVERSITY OF ILLINOIS Metz Ref Rm, Urbana IL; URBANA, IL (DAVISSON); URBANA, IL (LIBRARY); URBANA, IL (NEWMARK); Urbana IL (CE Dept, W. Gamble)
UNIVERSITY OF MASSACHUSETTS (Heronemus), Amherst MA CE Dept
UNIVERSITY OF MICHIGAN Ann Arbor MI (Richart)
UNIVERSITY OF NEBRASKA-LINCOLN Lincoln, NE (Ross Ice Shelf Proj.)
UNIVERSITY OF NEW MEXICO J Nielson-Engr Matls & Civil Sys Div, Albuquerque NM
UNIVERSITY OF NOTRE DAME Katona, Notre Dame, IN
UNIVERSITY OF TEXAS AT AUSTIN Austin TX (R. Olson)
UNIVERSITY OF WASHINGTON SEATTLE, WA (MERCHANT); SEATTLE, WA (OCEAN ENG RSCH LAB, GRAY); Seattle WA (E. Linger); Seattle, WA Transportation, Construction & Geom. Div
VIRGINIA INST. OF MARINE SCI. Gloucester Point VA (Library)
ATLANTIC RICHFIELD CO. DALLAS, TX (SMITH)
BECHTEL CORP. SAN FRANCISCO, CA (PHELPS)
BELGIUM HAECON, N.V., Gent
BETHLEHEM STEEL CO. Dismuke, Bethelehem, PA
BOUW KAMP INC Berkeley
BROWN & CALDWELL E M Saunders Walnut Creek, CA
BROWN & ROOT Houston TX (D. Ward)
CANADA Mem Univ Newfoundland (Chari), St Johns; Surveyor, Nenninger & Chenevert Inc., Montreal; Trans-Mnt

Oil Pipe Lone Corp. Vancouver, BC Canada; Warnock Hersey Prof. Srv Ltd, La Sale, Quebec
CF BRAUN CO Du Bouchet, Murray Hill, NJ
CHEVRON OIL FIELD RESEARCH CO. LA HABRA, CA (BROOKS)
FRANCE Dr. Dutertre, Boulogne; L. Pliskin, Paris; P. Jensen, Boulogne
GEOTECHNICAL ENGINEERS INC. Winchester, MA (Paulding)
GLIDDEN CO. STRONGSVILLE, OH (RSCH LIB)
HALEY & ALDRICH, INC. Cambridge MA (Aldrich, Jr.)
HONEYWELL, INC. Minneapolis MN (Residential Engr Lib.)
ITALY M. Caironi, Milan; Sergio Tattoni Milano; Torino (F. Levi)
LAMONT-DOHERTY GEOLOGICAL OBSERV. Palisades NY (McCoy); Palisades NY (Selwyn)
LOCKHEED OCEAN LABORATORY San Diego CA (F. Simpson)
MARATHON OIL CO Houston TX
MC CLELLAND ENGINEERS INC Houston TX (B. McClelland)
MOBIL PIPE LINE CO. DALLAS, TX MGR OF ENGR (NOACK)
MUESER, RUTLEDGE, WENTWORTH AND JOHNSTON NEW YORK (RICHARDS)
NEW ZEALAND New Zealand Concrete Research Assoc. (Librarian), Porirua
NORWAY DET NORSKE VERITAS (Library), Oslo; DET NORSKE VERITAS (Roren) Oslo; I. Foss, Oslo; J. Creed, Ski; Norwegian Tech Univ (Brandtzaeg), Trondheim
PORTLAND CEMENT ASSOC. Skokie IL (Rsch & Dev Lab, Lib.)
PRESCON CORP TOWSON, MD (KELLER)
RAND CORP. Santa Monica CA (A. Laupa)
RAYMOND INTERNATIONAL INC. E Colle Soil Tech Dept, Pennsauken, NJ
SANDIA LABORATORIES Library Div., Livermore CA
SEATECH CORP. MIAMI, FL (PERONI)
SHELL DEVELOPMENT CO. Houston TX (E. Doyle)
SHELL OIL CO. HOUSTON, TX (MARSHALL)
SWEDEN GeoTech Inst
TIDEWATER CONSTR. CO Norfolk VA (Fowler)
TRW SYSTEMS REDONDO BEACH, CA (DAI)
UNITED KINGDOM D. New, G. Maunsell & Partners, London; R. Browne, Southall, Middlesex; Shaw & Hatton (F. Hansen), London; Taylor, Woodrow Constr (014P), Southall, Middlesex
WOODWARD-CLYDE CONSULTANTS (A. Harrigan) San Francisco; PLYMOUTH MEETING PA (CROSS, III)
AL SMOOTS Los Angeles, CA
BARA, JOHN P. Lakewood, CO
BROWN, ROBERT University, AL
BULLOCK La Canada
F. HEUZE Boulder CO
LAYTON Redmond, WA
R.F. BESIER Old Saybrook CT
T.W. MERMEL Washington DC